ADVANCED MISSION PLANNING TOOL FOR REAL-TIME KINEMATIC (RTK) GPS SURVEYING

MICHAEL K. HOGAN

October 2001

TECHNICAL REPORT
NO. 211

ADVANCED MISSION PLANNING TOOL FOR REAL-TIME KINEMATIC (RTK) GPS SURVEYING

Michael K. Hogan

Department of Geodesy and Geomatics Engineering
University of New Brunswick
P.O. Box 4400
Fredericton, N.B.
Canada
E3B 5A3

October 2001

PREFACE

This technical report is an unedited reproduction of a report submitted in partial fulfillment of the requirements for the degree of Master of Engineering in the Department of Geodesy and Geomatics Engineering, July 2001. The research was supervised by Dr. Marcelo Santos, and support was provided by the Canadian Department of National Defence, the Communications Research Centre in Ottawa, and AWE Communications in Germany.

 The citation to this work should appear as follows:

Hogan, M. K. (2001). *Advanced Mission Planning Tool for Real-Time Kinematic (RTK) GPS Surveying*. M.Eng. report, Department of Geodesy and Geomatics Engineering Technical Report No. 211, University of New Brunswick, Fredericton, New Brunswick, Canada, 102 pp.

ABSTRACT

Conventional mission planning in GPS surveying involves locating a site with minimal obstructions and determining satellite availability at the location to be surveyed. Tools used in the planning process usually include topographic maps and satellite availability software. In recent years, with the advent of Real Time Kinematic (RTK) GPS surveying, it is possible to obtain centimeter-level accuracy while in the field. Applications for RTK GPS surveying include, but are not limited to: construction layout, land survey, photogrammetric survey control, and GIS updating.

One of the key factors in the RTK GPS technique is the data link between the reference station and rover. Without this link RTK GPS results are not attainable in the field. For this reason mission planning in RTK GPS surveying takes on another level of complexity: not only does the reference station have to visible to the satellites, but it must also be visible to the rover. However, available mission planning tools do not provide a means to predict the data link coverage of the reference station.

The purpose of this investigation is to determine the best wave propagation model or models to be used in an RTK GPS survey mission planning tool. This study will present current wave propagation models being used by communications planning software and then use these models to predict data link coverage. The performance of these models was evaluated through field testing of two RTK GPS systems.

This investigation concludes that there are three wave propagation models that could be used to accurately predict data link coverage by using only digital terrain information. The implementation of these models relies on available documentation and

potential source code. In researching this project, it was evident the availability of documentation varies between models. Based on performance criteria and implementation considerations, two models are recommended to be implemented into a mission planning tool for RTK GPS surveying: Parabolic Equation and TIREM.

ACKNOWLEDGEMENTS

I would like to acknowledge the financial support of the Department of National Defence in the completion of this project. I would like to thank my advisor, Dr. Marcelo Santos, for providing guidance and direction for the duration of this project. I would like to express my appreciation to Bob Stuart for his time and effort in completion of all field testing for this project. I would like to thank both the Communications Research Centre in Ottawa and AWE Communications in Germany for providing software and service support throughout the project. Finally, I would like to thank my wife, Anne-Renée, who has provided me with the love and support to see this project to completion.

TABLE OF CONTENTS

PAGE

LIST OF TABLES

MAIN BODY **PAGE**

LIST OF FIGURES

1

INTRODUCTION

The purpose of project described in this report was to investigate the use of wave propagation models for use as a mission planning tool for Real Time Kinematic (RTK) GPS Surveying. RTK GPS positioning is a differential technique that typically uses a combination of carrier-phase and pseudorange measurements and reference station coordinates broadcast from reference station to rover station where the processing of the rover data is carried out in real time [Langley, 1998]. RTK GPS surveying can obtain sub-centimetre results as long as the required number of satellites are in view of both reference and rover stations and there is a data link between the two.

In a surveying context, RTK GPS benefits many applications. Some of these include, construction layout (roads, pipes, and other utilities), GIS updating, topographic surveying, land surveying, photogrammetric control, and hydrographic surveying.

In any RTK GPS application, the two constraints for successful positioning are: visibility to the required number of satellites and a data link between the reference station and rover. Mission planning software tools have been developed by most GPS manufacturers that allow for predicting satellite visibility at a given location and time. As the local terrain and obstacles may affect the visibility of the satellite, these tools also allow for predictions with obstacles. Walker and Sang [n.d.] implemented accurate digital terrain models (DTM) with satellite visibility software to achieve a more realistic

prediction. The treatment of predicting the data link coverage between reference and rover by GPS manufacturers in the context of a mission planning tool is limited. Pacific Crest has published a document on data link applications [Pacific Crest Corporation, 2000] which includes the determination of the range of the data link. Walker and Kubik [n.d.] showed that a wave propagation model along with a DTM could be used for predicting communications in open pit mining.

Wave propagation models for the prediction of radio wave coverage from a given transmitter location have been of great interest for well over 60 years. These models have continued to be developed and improved along with computing power and boom in personal communications in the past 30 years. Today there are communications planning software tools that allow for prediction of radio wave coverage in all environments which take into account DTM, building databases, and land use/land cover (LULC) information. This software has been used in planning of many communications applications including television, radio, digital audio broadcasting, and cellular networks. Unfortunately, there are two main drawbacks to this type of software- the required expertise to properly use the software and the cost, which is in the order of $30,000.

Wave propagation models implemented into a mission planning tool have the potential to provide an RTK GPS user with site information that can save field time and expense. Cost and complexity inhibit taking advantage of the data link coverage predictions, by RTK GPS users, in the current form of communications planning software. Ideally a mission planning tool that incorporates readily available data link system information such as transmitting power, antenna gains, and system losses along with DTMs and LULC information would allow for an RTK GPS user to predict data

link coverage from a given location. This type of analysis would allow for a site to be evaluated based on the data link coverage or to evaluate the effect on coverage by modifying transmitting antenna heights or types. Furthermore, this type of mission planning tool would have to be inexpensive and relatively simple to use.

1.1 Project Objectives

The principal goal of this project is to determine the best wave propagation model or models for rural areas that incorporates readily obtainable radio system and terrain information to be used in RTK GPS survey mission planning and control network planning. The secondary objectives are:

1. Research wave propagation models being used in the current communications planning software.
2. Develop a field testing method to validate the models chosen.
3. Present criteria to compare the prediction results and the field measurements.
4. Make a recommendation of the best model to be implemented in a mission planning tool for RTK GPS surveying.

1.2 Motivation for Research

In 1999 the Construction Engineering Branch at Canadian Forces Base (CFB) Gagetown purchased an RTK GPS survey system. The intended use of this system is to

aid in maintaining a Geographical Information System, provide support to Base construction, provide support to Base Property Officer and Base Environmental Officer, and other required applications. CFB Gagetown is also responsible for various Army Reserve Armories in the Maritimes. The RTK GPS survey equipment will also be used to maintain any required geographical information of these sites.

CFB Gagetown consists of an area of approximately 1100 square kilometres and is divided into two main parts, Garrison and Training Area. The Garrison consists of approximately 10 square kilometres. Buildings, fields and roads similar to an urban environment occupy this land. One permanent control monument is set up to be used for RTK GPS surveying in the Garrison Area. The Training area is approximately 1090 square kilometres. The majority of the Training area is rural in nature. The terrain varies from 1 to 483 metres above mean sea level. Land cover consists of some built up areas, but is mostly tree covered or clear-cut. No permanent monuments required for RTK GPS surveying have been set up in the Training area.

Due to the size of CFB Gagetown, the one permanent control monument in place in the Garrison can not service the entire Base area for RTK GPS surveying. A control network is envisioned that would provide coverage for the entire Garrison and Training areas. The design of this network must take into account the characteristics of radio wave propagation.

1.3 Organization of Report

The report will be organized in the following manner:

Chapter 1 provides the context and summarizes the main goal the project. Along with this the secondary goals are presented and constraints of the project are outlined.

Chapter 2 summarizes the relevant background research including RTK GPS and mission planning. A description of the mechanisms affecting the propagation of waves at the VHF/UHF frequencies and simple wave propagation models are described.

Chapter 3 contains a brief description of the wave propagation models and communication planning software researched and used in the project. The field testing methodology is presented along with comparison criteria, which will be used to determine the best model for data link coverage prediction.

Chapter 4 presents the results from the field testing sessions and the model predictions. The criteria are used to compare the field testing results to the individual prediction results. The best models are compared to each other and recommendations are made.

Chapter 5 summarizes the project objectives and results of field testing and model prediction comparisons. The recommendation of the best model to be implemented is also stated. Finally topics for further research in this area are presented.

2

BACKGROUND

The purpose of this chapter is to provide the required background information for this report. Section 2.1 will discuss the Global Positioning System (GPS) and more specifically RTK GPS. Mission planning in GPS surveying and proposed RTK GPS surveying mission planning tool is presented in Section 2.2. Section 2.3 provides an introduction to communication systems and simple wave propagation models.

2.1 GPS Overview

Conceived in the 1970's, the Global Positioning System is the responsibility of the Joint Program Office (JPO) at the U.S. Air Force Systems Command's Space Division, Los Angeles Air Force Base [Hofmann-Wellenhof et. al., 1997]. Originally GPS was designed for military use, but under the direction of United States Congress and the President, civil use is promoted. GPS consists of three segments:

1. **Space Segment-** Consists of constellation of satellites broadcasting signals.
2. **Control Segment-** Consists of master control station, monitor stations, and ground control stations. The operational tasks of the control segment includes orbit and clock determination and prediction, time synchronization of satellites, and uploading of data to satellites.

3. **User Segment**- The user segment consists of both military and civilian users.

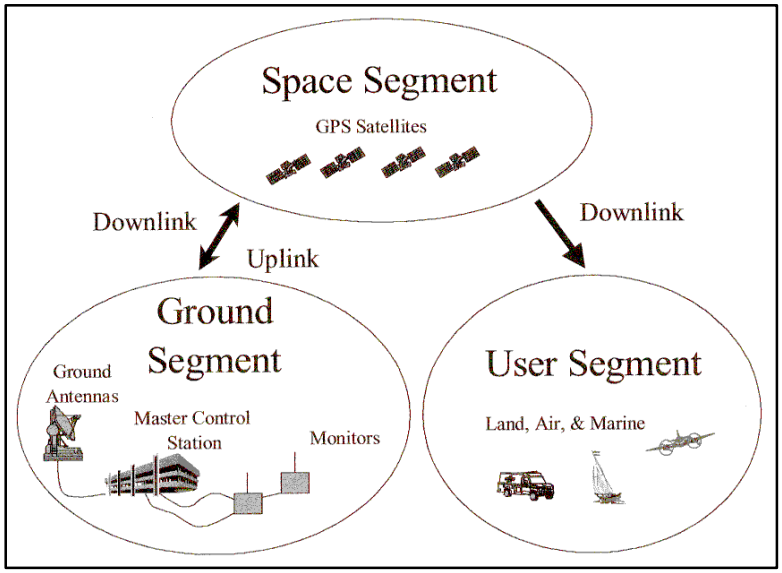

Figure 2-1: GPS Segments (from Varner [2000, p. 30]).

Figure 2-1 illustrates the three GPS segments. A detailed explanation of the segments can be found in any text describing GPS, for example, Leick [1990], Seeber [1993], or Hofmann-Wellenhof et al. [1997].

The modernization of GPS is currently underway and will continue for the next 20 years. Improvements include: discontinuing selective availability, which occurred in May 2000, enhancements to the control segment, and improvements to the signals being broadcast from the satellites. The modernizing of the signals include the addition of the C/A-code to the L2 frequency, new military signals on L1 and L2, real-time ionospheric delay corrections, more accurate satellite positions, velocities and time, and the addition

of a new civil frequency, L5. Descriptions of the modernization efforts can be found in Hatch et al. [2000], Sanhoo et al. [2000], and Van Dierendonck and Hegarty [2000].

2.1.1 GPS Positioning

Although originally conceived for military navigation purposes, GPS applications have become common place in all aspects of society. As the applications have developed so have techniques for using GPS technology. In surveying and navigation applications GPS techniques can be divided into two categories: standalone and differential (Figure 2-2).

Typically, standalone or point positioning using GPS involves the use of code pseudoranges either with Standard Positioning Service (SPS) or Precise Positioning Service (PPS). With Selective Availability (SA) incorporated the official accuracy of SPS is 100 m horizontally and 156 m vertically at 95% probability level and PPS can attain 16 m accuracy in the horizontal and 23 m in the vertical at 95% probability level [Hofmann-Wellenoff et.al., 1997]. Since discontinuing SA on May 2, 2000, a conservative estimate of SPS accuracy is 22 m horizontal and 33 m vertical at 95% probability level [Sandhoo et al., 2000].

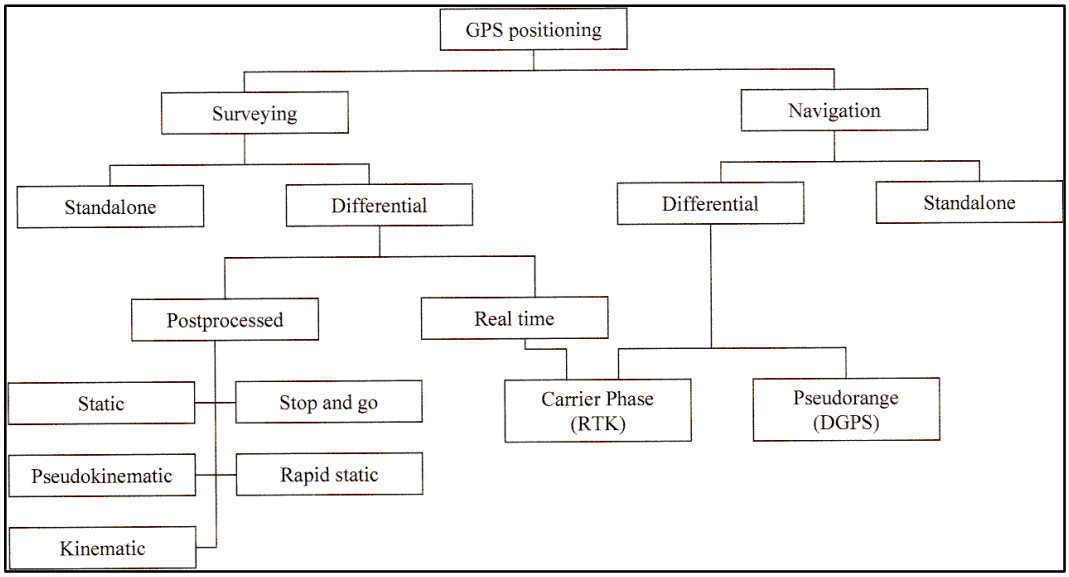

Figure 2-2: GPS Positioning Techniques [Langley, 1998].

Differential GPS is a technique that involves the use of two or more receivers: one reference or base receiver is located at a known position and the position of a remote receiver is to be determined. Differential GPS can be further divided into postprocessed and real-time. Various techniques of postprocessed differential GPS have been developed, but the most common for high-precision surveying is static processing. Real time differential positioning can be categorized as pseudorange and carrier-phase positioning. Pseudorange, which is commonly referred to as DGPS (Differential GPS), involves the broadcast of pseudorange and range rate corrections for each satellite in view from a reference station to rover receiver. DGPS will not be discussed further, but descriptions can be found in Parkinson and Enge [1996] and Hofmann-Wellenoff et al. [1997]. The real time carrier-phase positioning technique, which is commonly referred to

as Real Time Kinematic (RTK) positioning, is the main focus of this study and will be the described in the next section.

2.1.2 RTK GPS Technique

RTK GPS is classified as a differential GPS technique (Figure 2-2) that uses known coordinates of reference station to determine the coordinates of rover receiver. The technique typically uses a combination of carrier-phase and pseudorange measurements and reference coordinates broadcast from the reference station to the rover where the processing of the rover coordinates is carried out in real time [Langley, 1998]. Coordinates of the rover receiver can normally be determined at the centimeter level within a few seconds [Talbot, 1996; El-Mowafy, 2000]. Figure 2-3 illustrates the concept RTK GPS positioning technique. Both the reference and rover GPS antennas have the required number of satellites in view and there is a data link between the reference and rover receivers.

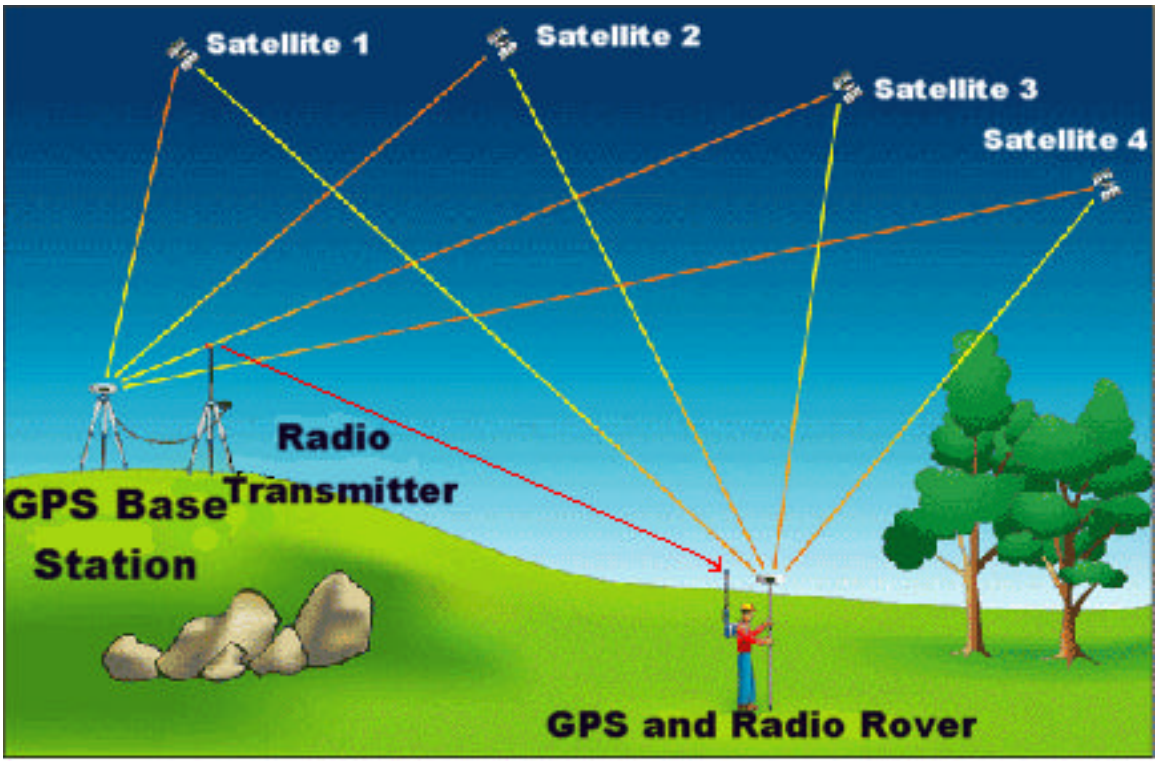

Figure 2-3: RTK GPS [Pacific Crest Corporation, 2001].

The components of RTK system include GPS receiver and antenna at reference and rover stations, radio transmitter at the reference station and radio receiver at rover station completing the data link between the two, and typically a handheld data collector. Figure 2-4 is a schematic diagram of the reference and rover station RTK GPS system components.

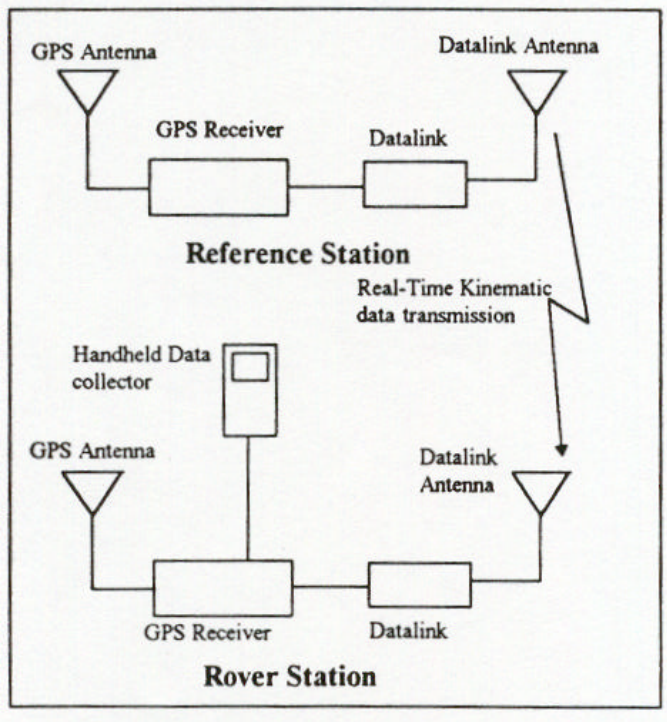

Figure 2-4: RTK system components (from Talbot [1996]).

2.1.2.1 RTK Data Link

The data link is an essential component of the RTK GPS system. RTK positioning requires regular transmission of data from the reference station to the rover. The rate of transmission is on the order of 0.5-2 Hz [RTCM, 1998]. Currently available data links in commercial RTK GPS survey systems take the form of a digital radio modem operating in the VHF or UHF frequency range [Trimble Navigation Limited, 1997; Pacific Crest Corporation, 1999; Magellan Corporation, 2000].

2.1.2.2 RTK Message Formats

The Radio Technical Commission for Maritime Services (RTCM) has devised a standard message format for dealing with RTK requirements as part of the RTCM Special Committee 104 (SC-104) format. According to RTCM SC-104 version 2.2 [RTCM, 1998] the RTK message formats consist of two message pairs. Message Type 18 and 19 contain uncorrected carrier-phase and pseudorange data, which can be used in differential processing (double-differencing algorithms). Message Types 20 and 21 contain corrections to carrier-phase and pseudorange and are not used as much as Type 18 and 19 [Langley, 1998]. The RTCM message formats are the most widely used, but proprietary formats such as Trimble's Compact Measurement Record (CMR) and Ashtech's Binary Data format have also been developed [Talbot, 1996; Langley, 1998; El-Mowafy, 2000]. Since RTK processing involves double-differencing of carrier-phase measurements at the rover receiver, the data update requirement is quite high.

2.1.2.3 Ambiguity Resolution

In order to take advantage of the centimetre level accuracy obtainable with RTK GPS the integer ambiguity, the unknown number of full cycles between satellite and receiver, of the carrier phase must be determined. This can be completed by field procedures such as occupying a known station (static initialization) or by On-The-Fly (OTF) initialization, which can be accomplished while stationary or moving [El-Mowafy, 2000]. As outlined by Langley [1998], the solution of the ambiguities is dependent on various factors, such as the number of satellites being tracked, use of pseudorange and carrier-phase data, observation noise, and use of single or dual frequency receiver. El-

Mowafy [2000] lists the follow ambiguity resolution techniques: Ambiguity Function Method (AFM), Least Squares Ambiguity Search Technique (LSAST), Fast Ambiguity Resolution Technique (FARA), Least Squares AMBiguity Deccorelation Adjustment (LAMBDA), Kim and Langley (1999) have also developed Optimal Method for Estimating GPS Ambiguities (OMEGA). Once initialization is gained in order to determine position at centimetre level accuracy, a minimum number of satellites must be tracked (usually four) and a constant data link between reference station and rover receivers must also be maintained.

2.2 GPS Mission Planning

Like any other survey application, GPS surveying requires pre-survey planning in order to increase the chances of a successful survey. The accuracy requirements of the specific project will determine the level of planning required. In general planning, a GPS survey consists of the following steps [Hofman-Wellenhof et al., 1997]:

1. **Mission Planning**- This is usually completed in the office and normally consists of two steps: site and observation window selection.
2. **Field Reconnaissance**- This step will ensure the actual site conditions meet the requirements from step one. For RTK surveys, factors affecting the data link between reference station and rover can also be evaluated.
3. **Monumentation**- Depending on the project requirements, the type of monument is selected and installed.

4. **Organizational Design-** This planning step involves determining occupation times, order of occupation, and who will occupy the specific site, if more than one crew is employed

The following sections will focus on the mission planning step and present the currently available mission planning tools.

2.2.1 Site Selection

NRC [1995] and Hofmann-Wellenhof et al. [1997] both suggest the use of large-scale topographic maps for plotting out desired survey points. Hofmann-Wellenhof et al. [1997] present four considerations in site selection process:

1. No obstructions above 20 degrees to avoid satellite signal blockage.
2. Avoid areas in the vicinity of reflecting surfaces to minimize multipath.
3. Avoid electrical installations to minimize signal disturbances due electromagnetic influence.
4. Proximity to road access to increase productivity.

Once the sites are selected the observation window can be determined.

2.2.2 Observation Window Selection

The determination of the optimum daily observation window (or period) is the next step in the mission planning process. Hofman-Wellenhof et al. [1997] define the

optimum window of satellite availability as the period when a maximum number of satellites can be observed simultaneously. Software planning tools provide graphical representation of the number of satellites visible in a given time period at a given location based on current GPS almanac information. These tools are usually provided by GPS software manufactures. However, the geometry of the GPS satellites is also an important factor in the accuracy of the position solution, therefore the Geometric Dilution of Precision (GDOP) gives a measure of satellite geometry. A GDOP under six is considered acceptable [Hofmann-Wellenhof et al., 1997]. The GDOP can be divided into components to look at specific aspects of the solution. These include: Position DOP (PDOP), Horizontal DOP (HDOP), Vertical DOP (VDOP), and Time DOP (TDOP) [Langley, 1999].

The first plot in Figure 2-5 is an example of the output from a satellite visibility program. The plot shows the number of available satellites (green) and PDOP (red). The spikes in the predicted PDOP values are associated with a low number of visible satellites during the given time period. The bottom plot in Figure 2-5 shows the PDOP and number of visible satellites for the same location and time, except with obstacles (tree stands) near the GPS antenna taken into account. The effect of the obstacles is reflected in the number of visible satellites and the respective PDOP values.

This type of analysis allows for the optimum window of observation to be determined and if a specific site is suitable for a GPS survey prior to starting the survey. The use of this type of tool is relatively simple and can be completed within minutes and has the potential to minimize time spent in the field by determining best time frame to collect data.

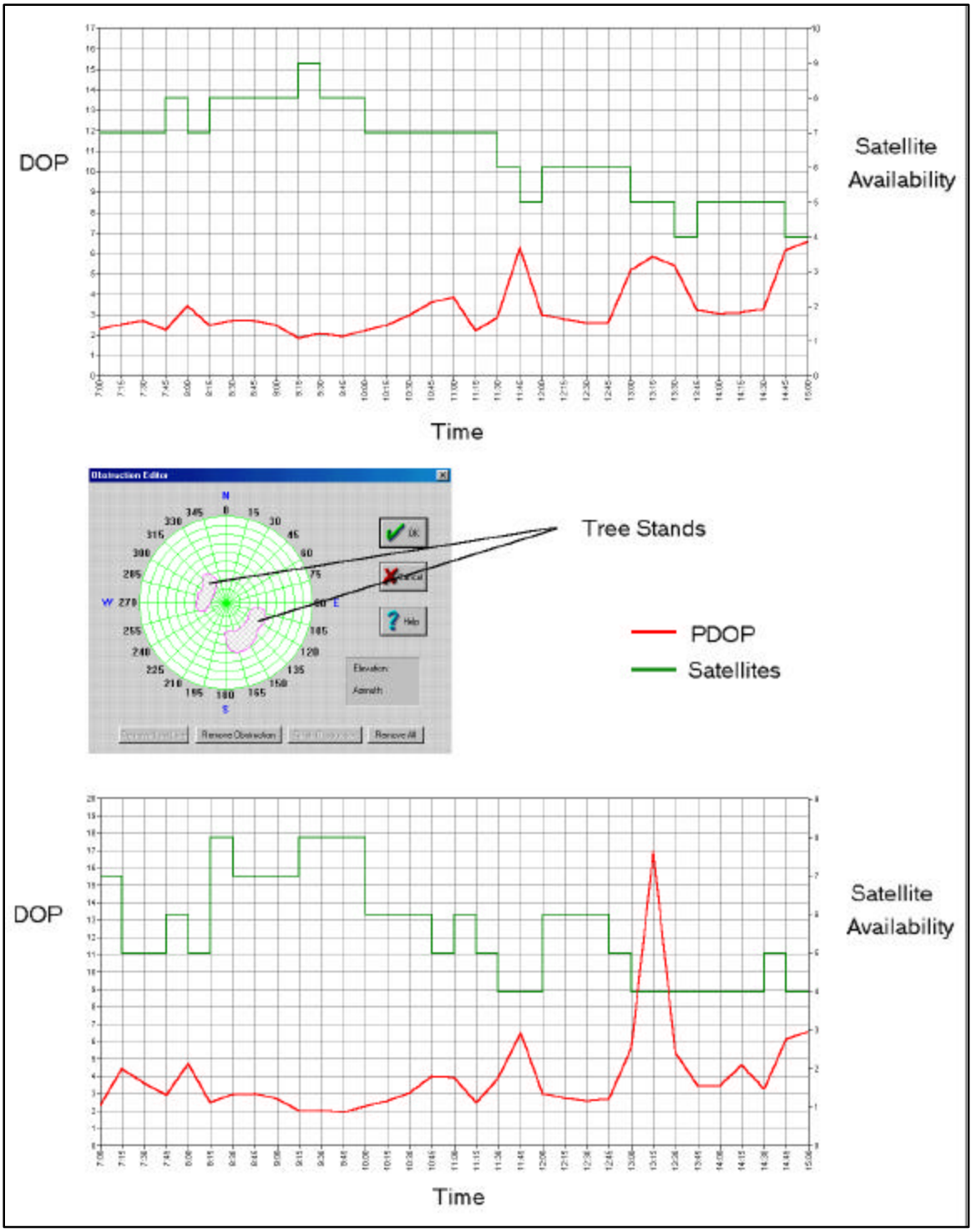

Figure 2-5: Satellite visibility and PDOP plots and the effect of obstacles near GPS antenna. Plots were created using Ashtech's Mission Planning software.

2.2.3 RTK GPS Mission Planning Requirements

As mentioned in the previous section, GPS mission planning tools provide the user with the ability to predict satellite visibility and DOP values for a given location and time, but tools to predict the data link coverage between reference and rover receivers are not available for the RTK user. However, Pacific Crest Corporation published a document [Pacific Crest Corporation, 2000] explaining the basics of radio wave propagation, link budge calculations, and predicted link distance. This document provides tips of how to maximize the coverage of the data link, including proper maintenance of radio equipment, frequency planning, and proper siting of reference station transmitting antenna. Once the RTK GPS equipment is purchased, the user has the control over choice of frequency (or channel) within licensing restrictions, siting of transmitting antenna, and to some extent the type of antenna.

2.2.3.1 Frequency Allocation

Frequency allocations are governed by federal and international agencies such as Industry Canada in Canada, Federal Communications Commission (FCC) in the United States, and the International Telecommunication Union. Frequencies available to be used for RTK applications include 150 to 174 MHz (VHF), 450 to 470 MHz (UHF), and Industrial, Scientific, and Medical (ISM) frequencies 902 to 928 MHz [Langley, 1998]. In planning an RTK GPS survey, the user has little control over the frequency, but within the allocated frequency range a channel can be changed if there is interference. For example, the Trimble Trimmark Base station transmitter operating in the 450-470 MHz range has a choice of 16 different channels [Trimble, 1998a].

2.2.3.2 Siting of Transmitting Antenna

In the planning of an RTK GPS survey the user has the most control over the siting of the data link transmitting antenna. Depending on the situation the user may or may not want to use existing control points, but either way data link coverage information is required in order to ensure the success of the survey. RTK GPS manufacturers recommend siting the transmitting antenna in a location that is high as possible and free of obstructions such as trees, buildings, hills etc. [Trimble Navigation Limited, 1998a; Pacific Crest Corporation, 2000]. The siting can be assisted by the use of topographic maps, as with static GPS mission planning, interpreting terrain through contours on the map. The determination of data link coverage can be difficult based on topographic maps, unless the user is familiar with the characteristics of the site and surrounding terrain.

2.2.4 Proposed RTK GPS Mission Planning Tool

A mission planning tool for RTK GPS surveying should provide a prediction of data link availability based on radio system and site characteristics, which may include terrain and land cover. The planning tool should include a measure of accuracy, for example, 95% probability that the signal will be available, and be easy to use. Figure 2-6 is a perspective view of a three-dimensional digital terrain model, increasing in height from green to brown, with a radio transmitter. Using this terrain model, a user may surmise based on the location of the transmitter that there could be areas where data link coverage is not available, but there is no guarantee of coverage.

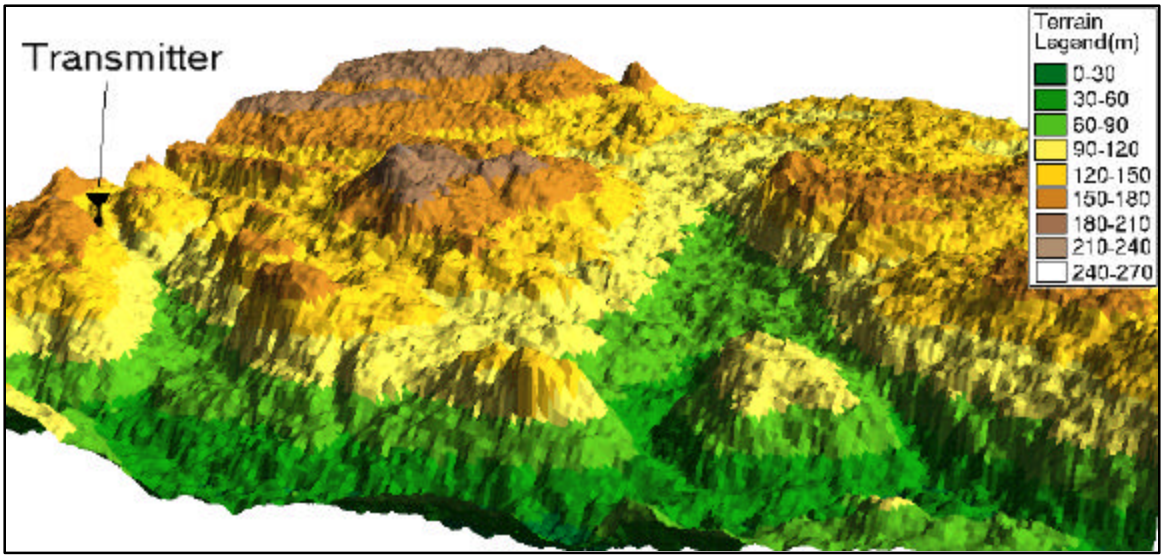

Figure 2-6: 3D Perspective of Digital Terrain Model.

Using this terrain model and readily attainable radio system characteristics the user can then use a radio wave prediction model to determine the data link coverage. Figure 2-7 is a prediction of the data link signal strength draped over the terrain model, the signal strength decreases from green to yellow to red.

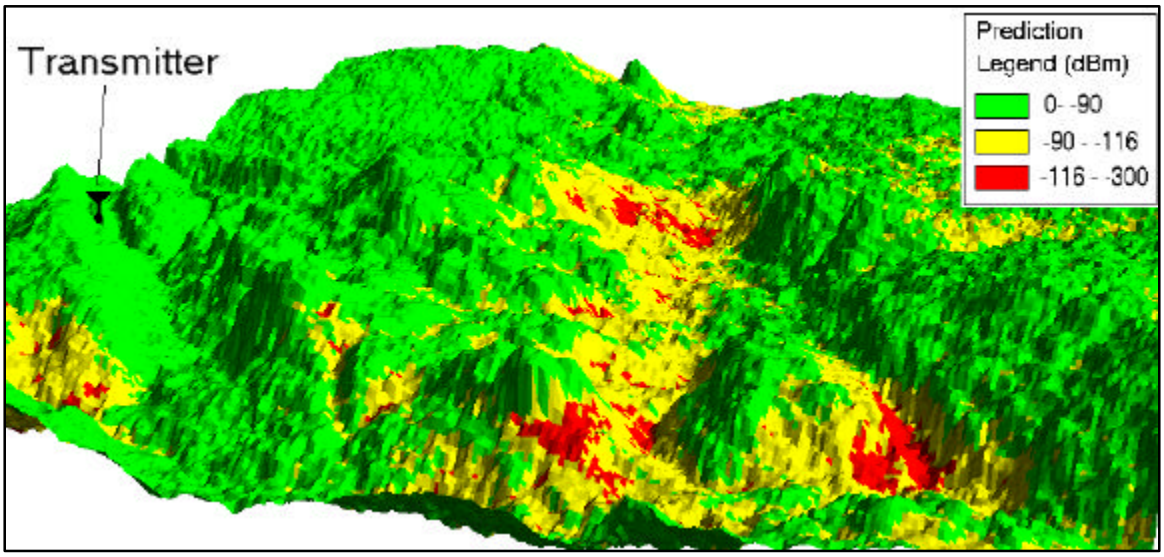

Figure 2-7: 3D Perspective of data link prediction draped over terrain model.

This type of prediction would provide the RTK GPS system user with important site characteristics in the office. The RTK GPS mission planning tool would allow the user to plan siting of RTK GPS data link transmitting antenna to ensure maximum coverage of the required area and minimize wasted field time due to data link outages.

2.3 Radio Communications

Assuming that both the reference and rover GPS receivers are tracking the minimum number of satellites, the key to the success of the RTK system becomes the communication between rover and reference station. The modeling of the propagation of radio waves in the VHF/UHF range over irregular terrain has been of interest for well over forty years [Egli, 1957] and has grown with the increased processing power of computers and the increase in personal wireless communications or cellular technology. This section will present the mode and the mechanisms affecting the propagation of radio waves in the VHF/UHF range. This section will also introduce several simple propagation models.

2.3.1 Mode of Propagation of VHF/UHF Bands

Parsons [1992] states the dominant mode of propagation of radio waves in the VHF (30-300 MHz) and UHF (300-3000 MHz) bands transmitted from relatively small antennas mounted close to the ground is the *space wave*. The space wave can be sub-divided into *direct waves*, which propagate in a direct path between transmitter and receiver and *ground-reflected waves* that reflect on the ground before arriving at the

receiving antenna. Figure 2-8 illustrates both components of the space wave in a simplified manner.

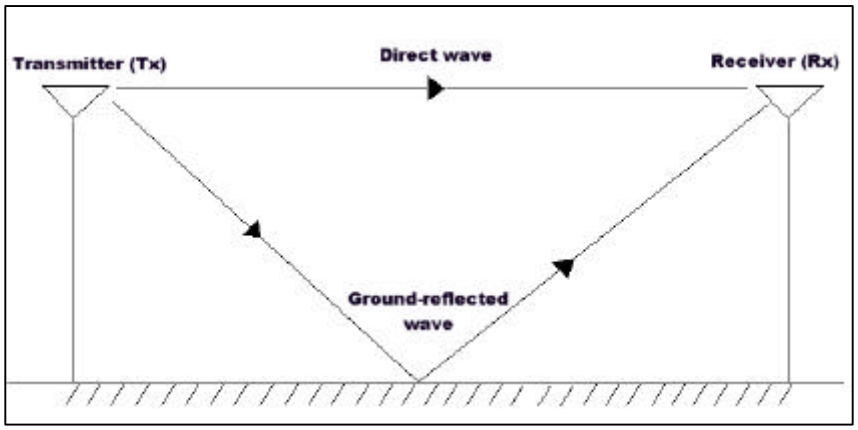

Figure 2-8: Components of the space wave

2.3.2 Mechanisms of Propagation

Rappaport [1996] and Parsons [1992] agree that the mechanisms involved in electromagnetic wave propagation are diverse, but there are three basic mechanisms that affect the propagation of radio waves in the VHF/UHF bands: reflection, diffraction, and scattering. Rappaport [1996] explains these propagation mechanisms as follows:

1. **Reflection** of a radio wave occurs when the wave impinges on an object that has very large dimensions compared to the wavelength of the propagating wave (VHF 1-10 m and UHF 0.1-1 m). Reflections can occur from the surface of the Earth or from buildings.
2. **Diffraction** of radio waves occurs when the path between the transmitter and the receiver has surfaces with sharp irregularities (edges). The resultant secondary waves from the irregular surface are present

throughout the space and behind the object, which gives rise to the "bending" of the waves. The bending of the wave can be described by Huygen's principle [Giancoli, 1985], which states that all points on a wavefront can be considered as point sources for the production of secondary wavelets, and that these wavelets combine to produce a new wavefront in the direction of propagation.

3. **Scattering** of radio waves occurs when small objects, relative to the wavelength, fall in the path of propagation between transmitter and receiver. Scattering of the radio wave can occur in the presence of foliage, street signs, and light posts.

2.3.3 Wave Propagation Models and Predicting Signal Path Loss

A propagation model is an empirical or mathematical expression used to compute the propagation path loss [IEEE, 1988]. If the radio system characteristics are known and the path loss is determined, the prediction of the received signal strength can be complete. Propagation models traditionally focus on predicting two components [Parsons, 1992; Rappaport, 1996]. These are:

1. *Average received signal strength at a given distance from the transmitter.* Typically the strength of the received signal is very small compared to the one transmitted, therefore it is expressed in decibels (dB). Either the voltage or power at the receiving antenna may be used. For this report the received signal strength will be expressed in terms of average power at the

receiving antenna (P_{ravg}). The received power is expressed in dBm (or dBmW), decibels relative to 1 milliwatt and

2. *Signal variability (s^2).* Determining the signal variability will allow the calculation of the probability if a specified signal level is available at a given location and time. This probability is known as the *coverage probability* [IEEE, 1988]. The area meeting the stated probability of receiving a signal exceeding the given level is called the *coverage area*. The specified signal level for this report will be the sensitivity of the data link receiver, which is the minimum signal strength that is "readable" by the receiver.

Propagation models can be broken down into two categories [Rappaport, 1996]: *large-scale* and *small-scale (or fading)*. Large-scale models predict the average received signal strength for an arbitrary transmitter-receiver separation. The term "large-scale" is used because the models characterize the signal strength over large transmitter-receiver (T-R) separation distances in the order of hundreds or thousands of meters. On the other hand, small-scale models characterize the signal strength over short distances (a few wavelengths) or a short time duration (a few seconds).

Figure 2-9 is an example of the received power against the T-R separation distance measured in the field. The large variations in the received power over short distances can be attributed to *fading*. According to IEEE [1983], fading is defined as the temporal variation of received signal power caused by changes in the transmission

medium or path. Rappaport [1996] describes fading as the rapid fluctuation of the amplitude of a radio signal over a short period of time or travel distance caused by interference between two or more versions of the transmitter signal arriving at the receiver at slightly different times. The received power may vary as much as three or four orders of magnitude (30-40 dB) when the receiver is moved by a fraction of wavelength. Small-scale models are used to predict this behaviour. Explanation of small-scale models can be found in Yacoub [1993] and Rappaport [1996], but will not be described further here.

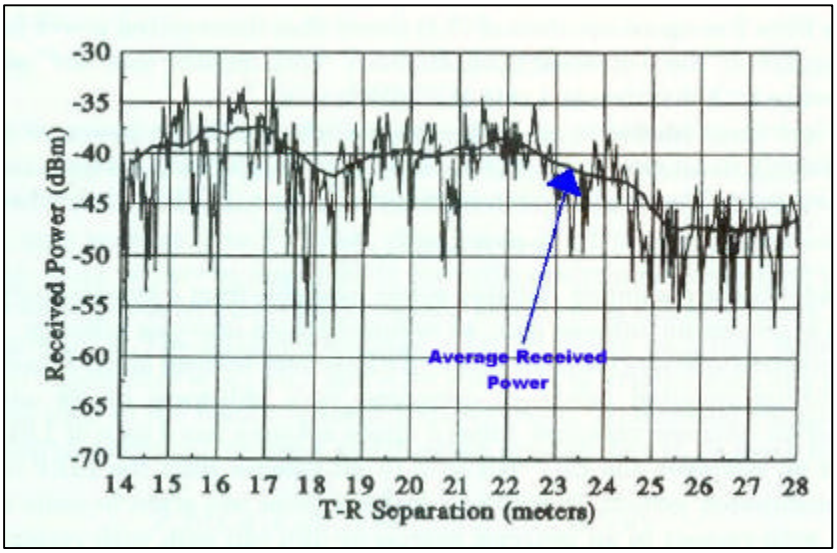

Figure 2-9: Small-scale fading and average received power (from Rappaport [1996, p. 71]).

As illustrated in Figure 2-9 the average received power, indicated by the arrow, gradually decreases as the receiver moves away from the transmitter. The average received power is determined from field measurements by averaging signal

measurements over a distance of 5 to 40 wavelengths [Lee, 1993; Rappaport, 1996]. The large-scale models are used to predict the average received power and will be the focus of this report.

2.3.3.1 Link Analysis

A link analysis is performed in the determination of the power received in a given T-R combination. In this process the system characteristics of the transmitter and receiver along with any loss of power due the path of travel are used to calculate the power available at the receiver. Figure 2-10 illustrates the simplified T-R combination.

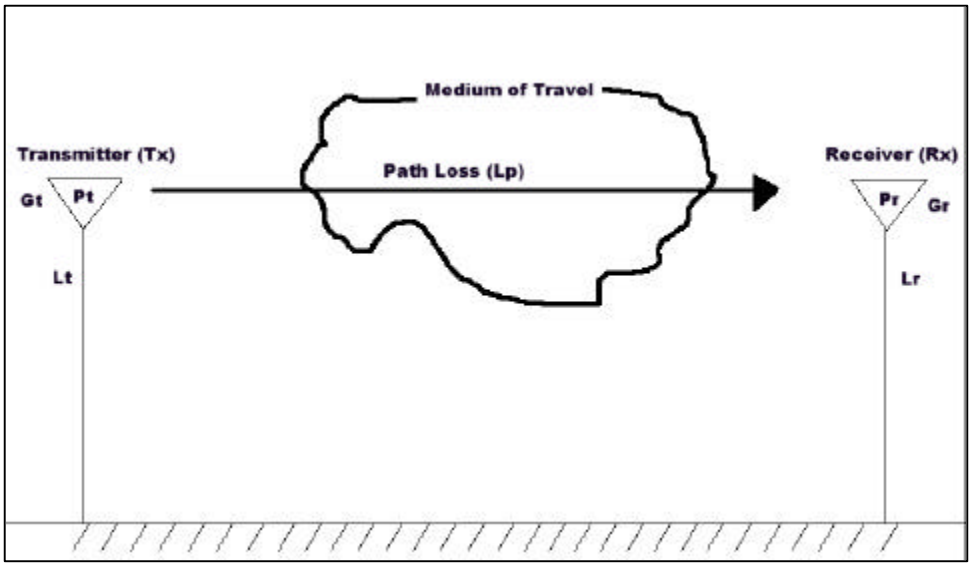

Figure 2-10: Simplified Transmitter/Receiver combination.

The parameters in this diagram are:

P_t = Power transmitted (dBm),

P_r = Power received (same as P_{ravg}) (dBm),

G_t = Gain of Transmitting Antenna (dBi),

G_r = Gain of Receiver Antenna (dBi),

L_t = System loss in Transmitter (dB),

L_r = System loss in Receiver (dB), and

L_p = Path Loss (dB).

Since these parameters are expressed in decibels, the received power can be determined through the arithmetic sum as follows:

$$P_r = P_t + G_t - L_t + G_r - L_r - L_p. \tag{2.1}$$

In the determination of the received power typically the L_t, G_t, P_t, G_r, and L_r are known for a particular system or can be determined from system manuals, therefore the path loss (L_p) is left as the only unknown. Path loss is defined as the attenuation undergone by an electromagnetic wave in transit between a transmitter and receiver [Federal Standard 1037C, 2000]. The path loss is a function of the medium and path of travel and the distance between the transmitter and receiver.

2.3.3.2 Basic Models

Strictly speaking, propagation models are used to predict the path loss, from which the received power can then be determined. Since the determination of path loss is critical to the design or analysis of a radio communications system various theoretical

models have been proposed. The following sections present basic prediction models that are only valid in specific circumstances. The theory behind these models is used to develop more complex models that can be employed to accurately predict the path loss in any given situation. The complex models used in this project will be described further in Chapter 3.

2.3.3.2.1 Free Space

The free space propagation model can be used to predict the received signal strength when a transmitter and receiver have a clear and unobstructed line-of-sight path [Rappaport, 1996]. The free space power received by an antenna is given by the Friis free space equation:

$$P_r\,(d) = (P_t G_t G_r \lambda^2)/(16\pi^2 d^2 L), \tag{2.2}$$

where P_t is the transmitter power and P_r (d) is the received power at some T-R separation distance (P_t and P_r are in the same units), d is T-R separation distance in meters, G_t and G_r are the gain of transmitting and receiving antennas respectively, L is the system loss not related to propagation, and λ is the wavelength in meters. Assuming no losses in the system hardware, L=1, the path loss for the free space is given as follows:

$$L_p\,(dB) = 10 \log_{10} (P_t/P_r) = -10 \log_{10} [(G_t G_r \lambda^2)/(16\pi^2 d^2)] \tag{2.3}$$

$$= -10 \log_{10} G_t - 10 \log G_r - 20 \log_{10} \lambda + 20 \log_{10} d + 21.984,$$

where L_p is in dB. As with other large-scale propagation models, the power decreases as function of the distance to some power. The free space model can be considered valid if there is clearance for the first Fresnel zone (Section 2.3.3.2.4), but in practice free space conditions are rarely encountered [IEEE, 1988].

2.2.3.2.2 Reflection

In the presence of a perfect conductor, a plane wave incident on the conductor will reflect all of its energy. As illustrated in Figure 2-11, the angle of incidence (θ_i) is equal to the angle of reflection (θ_r) and electric field (E_r) of a vertically polarized reflected wave is equal to the electric field (E_i) of incident wave.

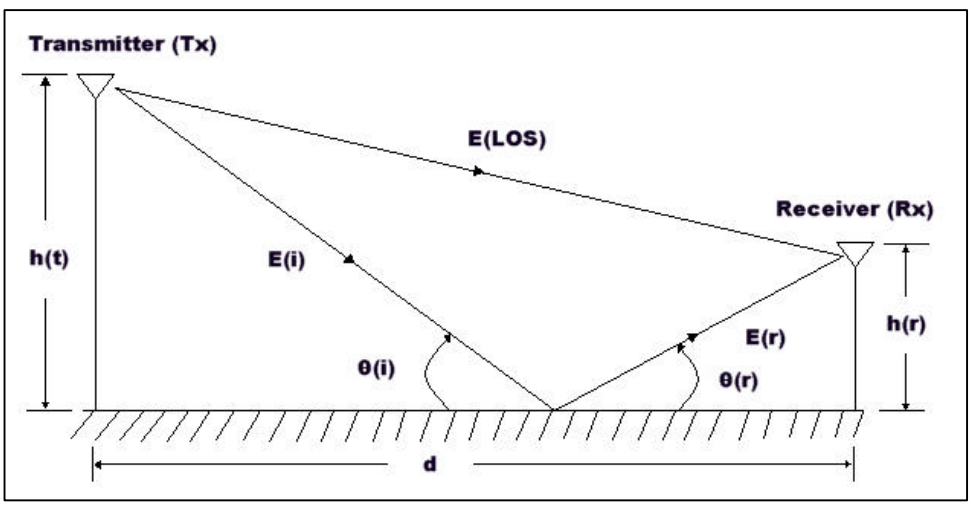

Figure 2-11: Direct and indirect paths for two-ray ground reflection model (from Rappaport [1996, p. 86]).

As mentioned in Section 2.3.3.2.1, the conditions for the free space model are seldom encountered, therefore a ground-reflection or 2-ray model based on geometric

optics can be used [Rappaport, 1996]. The 2-ray model takes into account both the direct and ground-reflected waves between the transmitter and receiver. Using Figure 2-11 and the assumption that the transmission path is limited to a few tens of kilometers, therefore plane Earth:

$$E_{Total} = E_{LOS} + E_r, \tag{2.4}$$

where E_{Total} is the total received electric field, E_{LOS} is the direct line-of-sight component, and E_r is the ground-reflected component. Assuming the ground is perfect conductor using equation 2.4 and the method of images the following equation for received power can be derived [Rappaport, 1996]:

$$P_r = (P_t G_t G_r h_t^2 h_r^2)/(d^4) \tag{2.5}$$

where h_t and h_r are the heights of transmitting and receiving antenna respectively, G_t and G_r are the gains of transmitting and receiving antennas, and d is the T-R separation distance. Based on equation 2.5 the transmitted power decreases inversely proportionally to the separation distance to a power of four and the received power is independent of frequency. Equation 2.5 can be expressed in decibels as follows:

$$L_p\,(dB) = 40 \log_{10} d - (10 \log_{10} G_t + 10 \log_{10} G_r + 20 \log_{10} h_t + 20 \log_{10} h_r\,). \tag{2.6}$$

The plane Earth model can be used when the terrain in the path of travel is considered smooth [Yacoub, 1993].

2.3.3.2.3 Refraction

In this situation space waves propagate very close to the Earth's surface and are usually limited to radio horizon. In theory, the radio horizon is greater than the optical horizon due to refraction of the waves in the atmosphere. Equation 2.7 [Coolen and Roddy, 1995] gives the maximum distance (d_{max}) a space wave can travel based on the radio horizon:

$$d_{max} = (2bh_t)^{1/2} + (2bh_r)^{1/2}, \tag{2.7}$$

where b is the fictitious radius of the Earth accounting for refraction, and h_t and h_r are the heights of transmitter and receiver respectively. Under standard atmospheric conditions the value of b is 1.33 times the radius of the Earth [Coolen and Roddy, 1995]. Using 6378.137 km as an average radius of the Earth and inputting the heights of transmitter and receiver in metres the radio horizon can be determined as follows:

$$d_{max} = 4.123\ [\ (h_t)^{1/2} + (h_r)^{1/2}\ ], \tag{2.8}$$

where d is in kilometers. This theoretical distance is difficult to attain in practice, since obstacles usually fall in the path between a transmitter and receiver that affect the propagation of the wave.

2.3.3.2.4 Diffraction

Diffraction of radio waves propagates them around the curved surface of the Earth and behind obstructions. Diffraction can be explained by Huygen's principle, which states that all points of a wavefront can be considered as point sources for the production of secondary wavelets, which combine to produce a new wavefront in the direction of propagation [Rappaport, 1996]. Fresnel zones can explain diffraction loss as a function of path difference. Fresnel zones are regions in space between successive ellipsoids of revolution with transmitter and receiver at the foci. The surface of the ellipsoids are defined by the condition that the combined distances from any point on the surface to the transmitter or receiver is greater than the direct distance by one-half of a wavelength. Figure 2-12 shows the nth Fresnel zone between transmitting and receiving antennas.

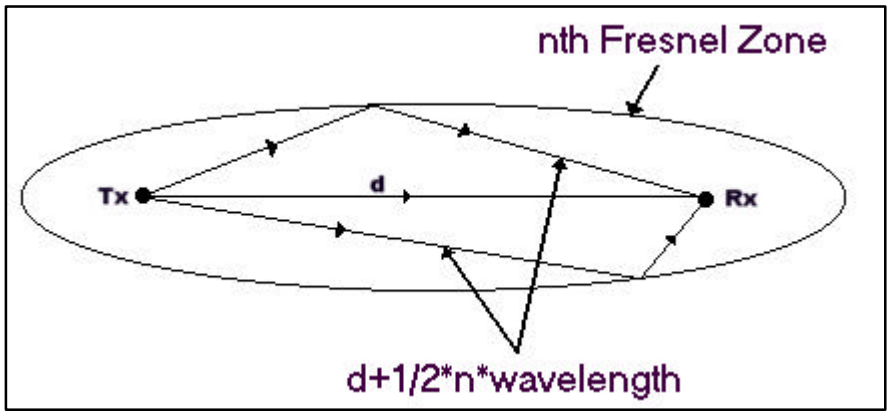

Figure 2-12: n^{th} Fresnel zone.

If path between the receiving and transmitting antennas does not have any obstructions, such as hills or buildings, in the region of the first Fresnel zone the diffraction loss will be minimal [Rappaport, 1996]. In most practical applications obstructions fall in the path between the receiving and transmitting antennas, therefore

various methods have been developed to model the diffraction loss. Descriptions of these methods can be found in Hess [1998], Parsons [1992], Yacoub [1993], Rappaport [1996], and Whitteker [1990].

2.2.3.3 Signal Variability

As discussed above, the propagation models predict the average received power (or more accurately the path loss) at a given distance from the transmitter, equally important in predicting the availability of a data link is the variability of the signal. This variation can be attributed to time and location. Since the location is the dominant factor, time variation can usually be neglected [IEEE, 1988]. Location variability has been shown to increase with frequency and terrain irregularity, but is not a function of T-R separation [Parsons, 1992]. Statistically, observations have shown that signal variation follows a log-normal distribution and is typically in the order of 4-10 dB [Parsons, 1992; Rappaport, 1996]. Table 2-1 lists the equations used to determine the signal standard deviation that have been proposed by various researchers and organizations.

Table 2-1: Equations for calculating typical signal standard deviation.

Author	Standard deviation (σ)	Reference
Egli	$\sigma = 5 \log_{10} f + 2$ dB	[Parsons, 1992]
Hufford and Montgomery	$\sigma = 3 \log_{10} f + 3.6$ dB	[Parsons, 1992]
Longley-Rice	$\sigma = 6 + 0.55(\Delta h/\lambda)^{1/2} - 0.004(\Delta h/\lambda)$ dB for $\Delta h/\lambda<4700$ $\sigma = 24.9$ dB for $\Delta h/\lambda>4700$	[Parsons, 1992]
CCIR (Comité Consultatif International de Radio)	10 dB Average terrain 15 dB Hilly terrain 18 dB Mountainous terrain	[Parsons, 1992]

In this table f is the frequency of the radio waves in MHz, λ is the wavelength in m, and Δh is the terrain irregularity parameter in m (described in Section 3.1.1.2).

2.2.3.4 Data Link Coverage

For any data link combination a location coverage probability must be stated as part of the design. Typically location coverage probability is in the order of 95-99% and would depend on the requirement. In a situation where reception of the signal must be received a high probability would be required, for example emergency communications.

3

PREDICTION MODELS, FIELD TESTING, AND COMPARISON CRITERIA

In order to determine the appropriate propagation model (or models) to be employed in the mission planning tool, coverage predictions and field validation must be carried out. This chapter will describe the specific prediction models used in this project and the associated communications engineering software, outline the field testing procedures, and propose the comparison criteria for the evaluation of wave propagation models.

3.1 Wave Propagation Models and Communication Planning Software

As part of the research for this project, wave propagation models used by current propagation software were investigated. The communications software investigated included: Probe from V-Soft Communications, CRC-COV from the Communications Research Centre, WinProp from AWE Communications Corporation, deciBel Planner from Northwood Technologies Limited, and TERPEM from Signal Science Limited. From this research and through price negotiation, two software packages were chosen for their specific models. The following sections will provide a brief description of the prediction models and the specific software used in this project.

3.1.1 Prediction Models Used in the Project

The models chosen have been developed and implemented in communications software packages in the past thirty years. Digital terrain information is an important part of each model, but how the respective model implements this information may vary. For example, the WinProp implementation of the Okumura-Hata model (Section 3.1.2.2) uses terrain information to determine the difference in height between the transmitter and receiver with respect to the terrain, whereas the Parabolic Equation takes a detailed terrain path between the transmitter and receiver into account. The goal of the following sections is to provide a brief introduction to each model. A more detailed explanation can be found in the respective references. It must be noted that the terminology and symbology is not consistent for each model.

3.1.1.1 Okumura-Hata

The Okumura-Hata (OH) model [Hata, 1980] is a set of empirical formulae based on measurements and analysis completed by Okumura [Okumura et al., 1968]. The model has been validated between 150 and 1500 MHz, with base station antenna heights of 30-200 meters, mobile station antenna heights between 1-10 meters, and separation distances from 1-20 kilometers. The basic formula is based upon urban areas, but has correction factor for both suburban and open areas. The OH model takes into account the heights of base and mobile antennas. According to Hata [1980], the following was taken into consideration during the formulation of the equations:

1. Propagation loss between isotropic antennas is treated.

2. Quasi-smooth terrain; irregular is not treated.

3. The urban area propagation loss is presented as the standard formula.

Equation 3.1 represents the urban prediction for path loss (L_{pu}):

$$L_p = 69.55 + 26.16 \log_{10} f_c - 13.82 \log_{10} h_b - a(h_m) + (44.9 - 6.55 \log_{10} h_b) \log_{10} R, \quad (3.1)$$

where L_{pu} in dB, f_c is the transmitting frequency in MHz, h_b is the base station height above the terrain in meters, h_m is the rover antenna height above the terrain in meters, and R is the distance between the transmitter and receiver in kilometers. Equation 3.2 is used to calculate the correction factor, $a(h_m)$, for a medium-small city:

$$a(h_m) = (1.1 \log_{10} f_c - 0.7)\, h_m - (1.56 \log_{10} f_c - 0.8). \quad (3.2)$$

The path loss for open areas (L_{po}) is determined using equation 3.1, 3.2, and a correction factor as follows:

$$L_{po} = L_{pu} - 4.78 (\log_{10} f_c)^2 + 18.33 \log_{10} f_c - 40.94. \quad (3.3)$$

At a given frequency and transmitter and receiver height combination, the path loss using the OH model becomes a function of the distance between the transmitter and receiver, R.

3.1.1.2 Longley-Rice

The Longley-Rice (LR) model was first presented in 1968 in the ESSA Technical Report [Parsons, 1992]. The model predicts the mean path loss relative to the free space loss and requires parameters such as frequency, heights of the transmitting and receiving antennas, distance between antennas, mean surface refractivity, Earth's conductivity and dielectric constant, polarization and description of the terrain [Yacoub, 1993]. The model is a computer-based algorithm that has been validated between 20 MHz and 20 GHz, antenna heights between 0.5 and 3000 metres, T-R separation from 1 to 2000 kilometers, and vertical or horizontal polarization.

When a digital terrain model is available the LR model will extract terrain profiles between the transmitter and receiver. These profiles are used to determine the distance, radio horizon, the horizontal elevation angles, and effective antenna heights. A detailed description of these parameters can be found in IEEE [1988] and Parsons [1992].

Another parameter used by the LR model is the terrain irregularity parameter, Δh, which is an indicator of the terrain roughness or undulation. Assuming a normal distribution of the terrain over a given distance, the terrain irregularity parameter is estimated as the distance between the 10 and 90 percent ranges of the average. This is illustrated in Figure 3-1. Table 3-1 lists estimated values of Δh for different types of terrain.

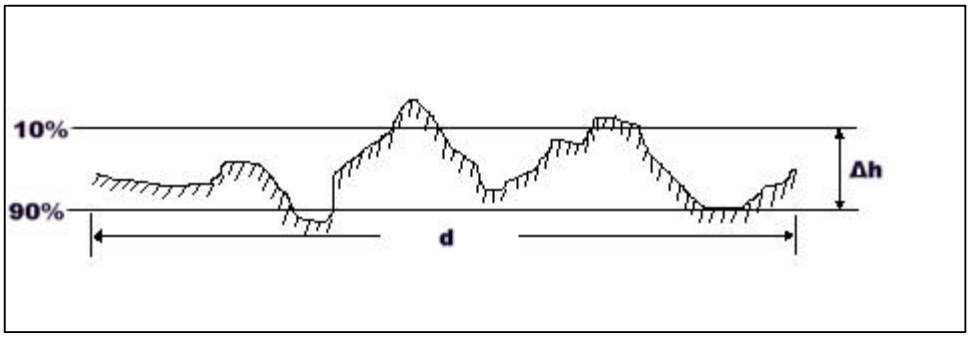

Figure 3-1: Terrain irregularity parameter (from Yacoub [1993, p. 77]).

Table 3-1: Estimated values Δh (from Yacoub [1993, p. 78])

Type of Terrain	Δh (metres)
Water or very smooth terrain	0-5
Smooth terrain	5-20
Quasi smooth terrain	20-40
Rolling terrain	40-80
Hills	80-150
Mountains	150-300
Rugged Mountains	300-700

The method for calculation of the average path loss using the LR model depends on the separation distance between the transmitting and receiving antennas [Parsons, 1992]. Depending on the distance, the model uses free space, plane Earth, and single or double knife-edge diffraction loss. Descriptions of knife-edge diffraction loss can be found in Parsons [1992], Yacoub [1993], and Rappaport [1996].

3.1.1.3 TIREM

The Terrain Integrated Rough Earth Model (TIREM) was developed by the office of the United States Department of Commerce, National Telecommunications and

Information Administration [IEEE, 1988]. TIREM predicts propagation loss between two points by taking into account the transmitting frequency, atmospheric and ground parameters (ground permittivity and conductivity), and the terrain profile between the transmitter and receiver. The model is valid between 40 MHz and 20 GHz. The range of valid antenna heights was not given.

The calculation of the average path loss is complete for radio line-of-sight (or radio horizon) paths and for beyond line-of-sight paths. For line-of-sight paths the computation depends on the minimum ratio, along the entire path of the ray, of terrain clearance height, h, and the dimensions of the first Fresnel zone, r, at that point. These parameters are illustrated in Figure 3-2.

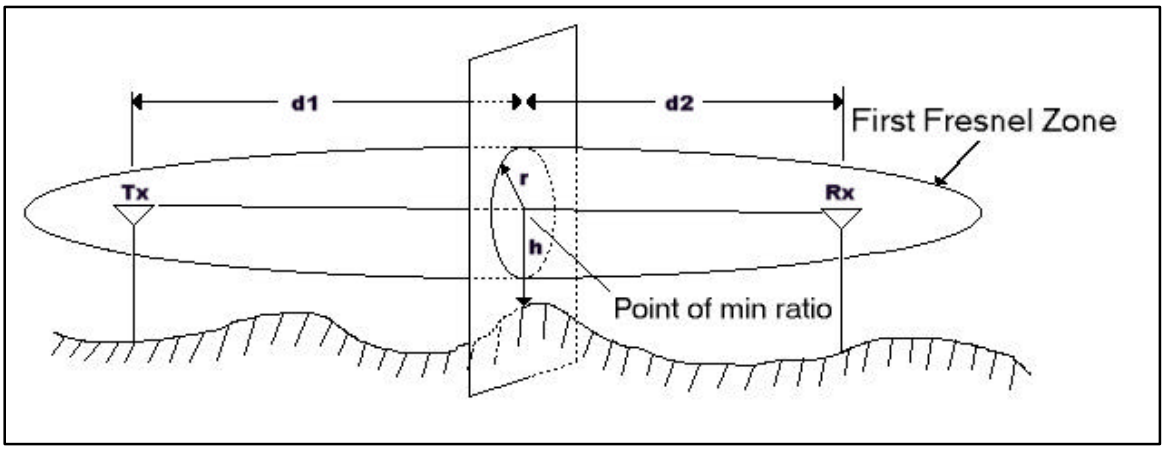

Figure 3-2: Line-of-sight parameters for TIREM model [IEEE, 1998].

Table 3-2 lists the modes of calculation for line-of-sight paths.

Table 3-2: TIREM line-of-sight modes [IEEE, 1988].

h/r 1.5	The ray is well above the terrain and free space loss is used
h/r 0.5	The ray is very near the earth's surface, and an empirical rough-earth formulation is used to compute the loss.
0.5 < h/r < 1.5	A weighted combination of free-space and rough-earth losses is used.

Beyond the line-of-sight there are nine different propagation modes that are used [IEEE, 1988]. These include knife-edge diffraction, double knife edge diffraction, rough-earth diffraction, tropospheric scatter, or a combination of these.

3.1.1.4 CRC Predict

The CRC Predict model was developed at the Communications Research Centre (CRC) in Ottawa. The model has been validated for transmitting frequencies between 30 and 3000 MHz, transmitting antenna heights between 30 to 200 metres, and receiving antenna heights between 1 to 10 metres [Chouinard et al., 1996]. The calculation of path loss is completed by calculating the loss due to diffraction [Whitteker, 1990] and tropospheric scatter [CRC, 1996] using terrain and land cover information. Diffraction loss is based on numerical integration and takes into account all terrain between transmitter and receiver. The integration is completed in both directions and the weighted average is taken for the solution [CRC, 1996]. The theory behind the CRC Predict model can be found in Whitteker [1990] and [1994] and a description of the Predict algorithm can be found in CRC [1994].

3.1.1.5 Parabolic Equation

The foundation of the parabolic equation for modeling waves lies in Maxwell's equations, a detailed description of which can be found in Feynman et al. [1964], and solutions to the partial differential equations formed by Maxwell's equations. The three dimensional (x, y, z) partial differential wave equation in free space can be written as follows [Feynman et al., 1964]:

$$\partial^2\mathbf{E}/\partial x^2 + \partial^2\mathbf{E}/\partial y^2 + \partial^2\mathbf{E}/\partial z^2 - c^{-2}\partial^2\mathbf{E}/\partial t^2 = 0, \tag{3.4}$$

where **E** is the electric field, t is time, and c is the vacuum speed of light.

The terminology "parabolic", comes from the classification of partial differential equations and an analogy to the quadratic equation in analytic geometry [Myint-U, 1980]. Given the following quadratic equation:

$$Ax^2 + Bxy + Cy^2 + Dx + Ey + F = 0, \tag{3.5}$$

the solution is hyperbolic, parabolic, or elliptical if $B^2 - 4AC$ is positive, zero, or negative respectively.

The PE was first introduced in the 1940s, but with the advent of the digital computers the use of the PE has increased [Levy, 2000]. The use of the PE has been proposed for many circumstances including: oversea and tropospheric propagation. Of primary interest for this project is the propagation of radio waves over irregular terrain.

Descriptions of various implementations of the PE over irregular terrain can be found in Dockery [1988], Levy [1990], Kuttler and Dockery [1991], and Levy [2000].

3.1.2 Communications Planning Software Used in Project

As previously mentioned various communications planning software were investigated for this project. The software packages were chosen due to the variety of models used and both organizations authoring these packages have their foundations in research. The following sections provide a brief description of the software used in this project and any specific model implementation details. Through discussions with the respective representatives of the organizations and through explaining the nature of the this project, these models were recommended for this investigation.

3.1.2.1 CRC-COV: Communications Research Centre

The Communications Research Centre (CRC) in Ottawa, which is a government agency of Industry Canada, developed CRC-COV software. CRC-COV and the updated version, CRC-COV Lab, are used to design and predict coverage of broadcast systems. These are well-developed software packages that take into account advanced system parameters such as antenna patterns and multiple transmitters, environmental factors, and various terrain databases [CRC, 2001]. The estimated cost of the CRC-COV Lab is $25,000 (CDN). The specific models from CRC-COV used for this project were: Okumura-Hata, Longley-Rice, TIREM, and CRC-Predict.

3.1.2.2 WinProp: AWE Communications Corporation

AWE Communications Corporation is a spin-off from the Institute of Radio Frequency Technology at the University of Stuttgart in Germany. The main focus of this company is the development of software tools for radio network planning and wave propagation [AWE, 2001]. The software can be used for rural (macrocell), urban (microcell), and indoor (picocell) propagation. The software is modular in nature and specific components can be purchased for particular scenarios (i.e. indoor propagation). The cost of the software is approximately $33,000 (CDN) for all modules and $4,000 (CDN) for the urban module required for this project. The specific models from WinProp used in this project were Okumura-Hata and Parabolic Equation.

The implementation of the Okumura-Hata model is similar to that explained in Section 3.1.1.1. AWE communications has introduced a variable called h_{eff} (effective antenna height), which is the height difference between transmitter and receiver, to account Hata's assumption of flat terrain. This variable replaces h_b in Equation 3.1, otherwise the implementation is similar to the Okumrua-Hata method. Implementation details of the PE can be found in AWE Communications [n.d. b] and [n.d. c]; unfortunately these documents are not available in English.

3.2 Field Testing of Data Link

Field testing must be carried out to confirm the predictions provided by the models discussed in Section 3.1. The proposed field testing of the data link employs the RTK GPS equipment in the measurement process. The benefits of using the RTK GPS

equipment include: the accurate positioning of antenna for each measurement, the testing mirrors the actual RTK GPS survey process, and the measurement process is kept simple. The main drawback of using the RTK GPS equipment is the signal strength can not be measured directly, which may affect the comparison to the predictions.

The proposed testing methodology can be broken up into three steps: map reconnaissance, control survey, and data link testing. Each step will be described in the following sections.

3.2.1 Map Reconnaissance

This phase consists of studying topographical and terrain maps of the training area at CFB Gagetown as well as consulting Base staff to determine suitable locations for reference station location. Factors affecting the choice of reference station location include:

1. **Surrounding terrain**- The variation of the terrain surrounding the reference station must be sufficient to ensure the transmitter signal is degraded or completely lost.
2. **Test route**- The test route must be within the optimum range of the transmitter as suggested by specifications. This will ensure that the effects on the received signal strength are due to the local terrain and not distance from transmitter.
3. **Access**- Road access surrounding the reference station must be sufficient to allow for testing in different directions. Due to military training, access to certain areas may be restricted.

3.2.3..... Field Reconnaissance and Control Survey

This phase consists of physically viewing the sites specified in the Map Reconnaissance and placement of a temporary control monument at the acceptable sites. The position of the control point, if not known, will be determined by GPS static survey. The postprocessing of the GPS data will be completed with GPS data from the CE base station GPS receiver.

3.2.3 Data Link Testing

The devised testing method is limited to the use of the Trimble survey equipment available at UNB and CFB Gagetown CE Section, specifically the Trimble 4700 and the Trimble 4800. Using the output on the data logger LCD readout and the modes of the Trimble RTK surveying (fixed, float, and autonomous) a measurements scheme was devised. When there is a data link between reference station and rover an icon appears on the LCD readout of the data logger. This icon may flicker, on and off, during the survey. If radio communications are lost between the reference and rover stations a warning appears stating “data link down”. The modes for RTK surveying of the Trimble systems are as follows:

1. **RTK Fixed**- This mode, as indicated on the data logger, means that there is initialization between the reference station and rover. Centimetre level positioning is possible.
2. **RTK Float**- This mode, as indicated on the data logger, means that initialization has not been gained or it is lost between the reference station

and rover. A float solution may occur if the number of visible satellites falls below four. Submetre level positioning is possible.

3. **Auto**- This mode, as indicated on the data logger, means that the data link has been lost between the reference station and rover. The rover GPS receiver will be making measurements as a stand alone receiver. Positioning consistent with SPS is possible.

Based on the RTK modes, the data link icon that appears on the data logger, and the warning message, the following measurement scheme for the data link at each RTK observation is proposed:

1. **GREEN**- If from the last measured point the radio link icon did not go on and off and the position is determined with fixed or float solution. Green would assume that there is no interference with the radio link between the reference and rover.
2. **YELLOW**- If from the last measured point the radio link icon went on and off or the warning appears, but the position is determined with fixed or float solution. Yellow would be a warning that there may be potential for interference with the radio link, but positioning is still available.
3. **RED**- If from the last measured point the radio link icon went on and off or the warning appears, and the position is determined in autonomous mode. When Red is used there is no link between the reference and rover and RTK GPS positioning is not available.

Using the measurement scheme outlined above, the following steps were proposed for testing of the data link:

1. Set up the GPS base station and the radio transmitter on one of the control points determined in Step 2, field reconnaissance and control survey.
2. Set up the rover receivers on the test vehicle.
3. Set both receivers in RTK mode and initialize with reference station.
4. Drive pre-determined test routes taking positioning observations depending on terrain and availability of the radio link. For example, distances between observations may be decreased if the signal is variable or it is evident by the terrain, that the signal may be affected.
5. RTK observations are classified by color.

This testing procedure should be completed on the same test routes at different times to provide redundancy in the measurements.

3.3 Comparison Criteria

In order to compare each prediction model investigated in this project to the field measurements, the performance criteria were proposed. Performance criteria refer to how the model predictions performed compared to the field measurements. The three criteria are: visual comparison, route profile analysis, and coverage probability comparison. Each of these will be explained below and then used in Chapter 4.

3.3.1 Visual Comparison

The visual comparison consists of analysing plan view plots of two layers of data, prediction and field results. Depending on the sensitivity of the receiver, the predictions are classified using the colours of green, yellow, and red. This type of representation will allow for an intuitive analysis of how the predictions are affected by the terrain. For example, does the prediction make sense when compared with local terrain?

3.3.2 Route Profile Analysis

This analysis looks at the predicted results against the field measurements along the drive test route. The predicted field strength is typically given in dBm, but the field measurements are colour coded. For these reasons, constant values (in dBm) are assigned to each colour, for this project the constant values will be associated with the sensitivity of the receiver and legend of prediction results. This type of analysis will highlight the trends in both the predictions and field measurements and allow for a correlation between the model and field test to be determined.

3.3.3 Coverage Probability Comparison

For this comparison, three elements are required for each field measurement: predicted average received power, the associated standard deviation, and sensitivity (specified signal level) of the receiver. A coverage probability must be chosen: typically this is in the order of 95-99%. From these a statistical comparison can be made between the field measurement and the corresponding prediction. For example, if the field

measurement is green and the probability of the corresponding predicted value is greater than the sensitivity, then there would be a positive correlation.

4

RESULTS AND ANALYSIS

This chapter will present the results of the field tests in Section 4.1. Section 4.2 presents the results from the six prediction models described in Chapter 3. The field test results are compared to the predictions in Section 4.3. Section 4.4 summarizes and compares the best models from the previous sections. Recommendations are made based on the results and considerations for implementation of the respective model.

4.1 Field Testing Results

The first two steps of the field testing from section 3.2.3 were completed on the 21st and 22nd of August 2000. Two sites were chosen for further investigation to be used as control, Knowlton Hill and Headline Hill. These two sites were visited and occupied with GPS antenna and receiver for static baseline positioning. The data were postprocessed with CE base station data to determine the positions of the points. The following sections will describe the chosen test area and present the results from the field testing.

4.1.1 Test Area and Route Tested

Using the method described in Section 3.2.3 drive tests were carried out on two separate occasions. The first session was carried out on the 23rd and 24th of August 2000 and the second session was carried out on the 4th of November 2000. The first day of session one consisted of practicing drive test methodology and determining which

reference station location and surrounding area would provide the best test area. Through this process, it was determined that the Headline Hill location and surrounding area was best for the drive testing, since the area showed a high degree of variation in the received signal strength well within the limits of the RTK GPS system. The respective locations of the test area and drive test route within CFB Gagetown are illustrated in Figure 4-1. The test area was approximately 9 x 11 km. The terrain in the test area varies in height between 15 and 220 m above mean sea level.

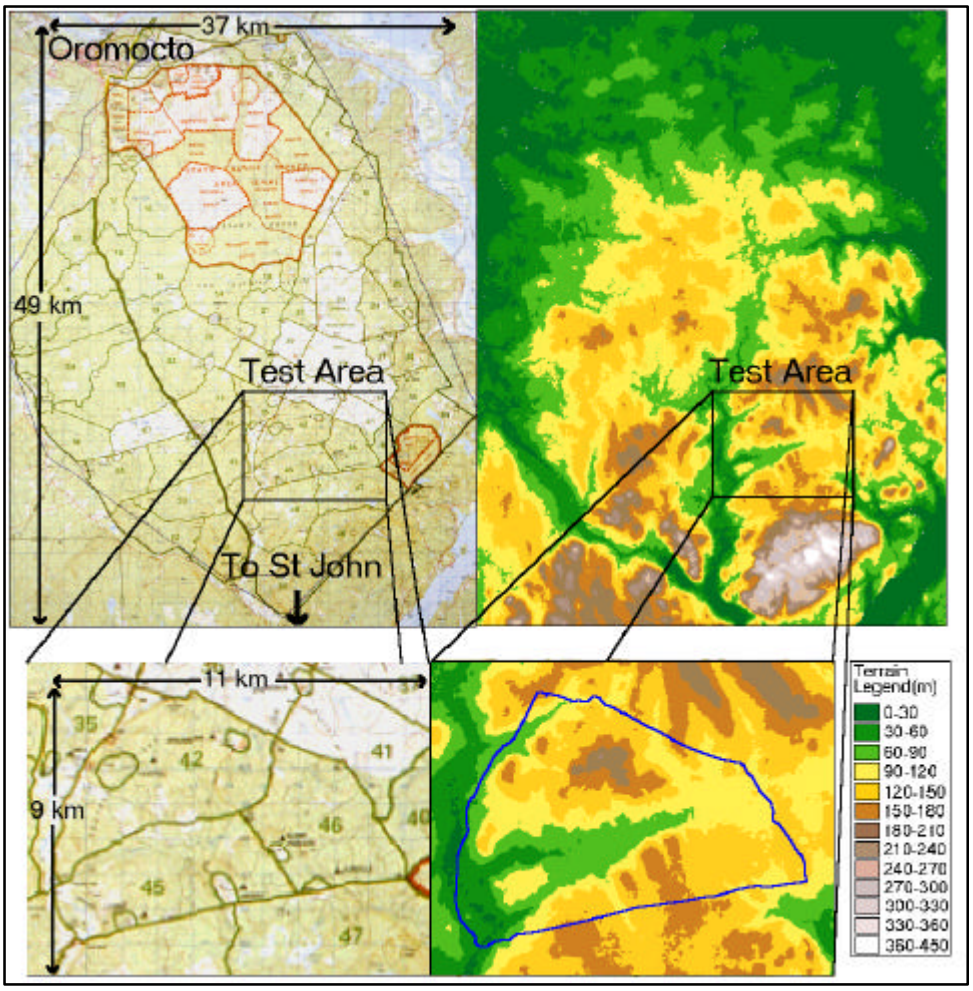

Figure 4-1: Map of CFB Gagetown and corresponding DTM.

Figure 4-2 shows a terrain model and aerial photograph of the test area. The concentric circles represent 5 and 10 km distances from the Headline Hill reference station. The arrow indicates the direction driven during the tests. The drive test route (marked in blue) was circular in nature starting and ending at the Headline Hill reference station, as illustrated by Figure 4-2.

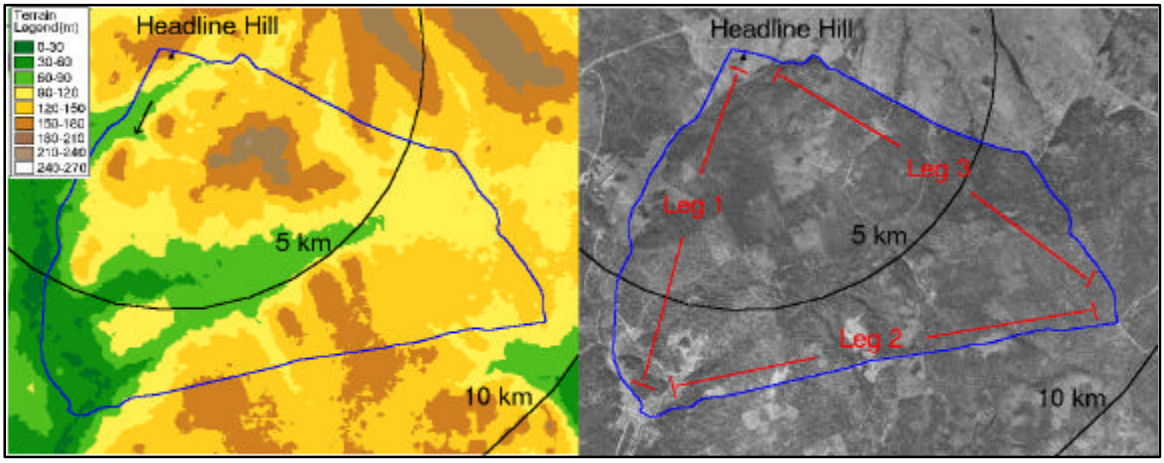

Figure 4-2: Testing and Route overlaid DTM and Aerial Photograph.

The total length of the route was approximately 28 km and can be broken down into three legs. The first leg of the route is radial from the reference station and approximately 8 km long. The terrain for this leg decreases down to 20 m along the route. The second leg of the route is approximately circumferential to the reference station and is approximately 10 km long. The terrain for this leg varies between 30 to 170 m along the route. The third leg of the route is also radial and returns back to the reference station. The length of this leg is 10 km and the terrain along the route varies between 90 and 155 m. As indicated in Figure 4-2 there is a large hill near the centre of

the area circumscribed by route approximately 2.5 km from the reference station with the peak reaching 220 m above mean sea level. Directly behind the hill, with respect to the reference station, is a valley.

Figure 4-3 shows the 2 km marks along the drive test route and a terrain profile along the route. Also included in the terrain profile is the maximum height along a radial profile (stars) from transmitter to 1 to 24 km marks along the route at 1 km spacing. From this, we see that the height of the terrain at specific locations between the transmitter and route varies between 25 to 125 m greater than that of the route height.

The testing of the radio link using this route was complete during each session. The first test was on the 24th of August 2000 and the second was on the 4th of November 2000. The labeling of these tests will be “Survey 1” and “Survey 2” respectively for the remainder of this report. As indicated earlier two RTK GPS systems were employed on the vehicle, Trimble 4700 and 4800, which will be labeled simply “4700” and “4800” for the remainder of this paper. Survey 2 was approximately 4 km shorter than Survey 1 due to time constraints. For this reason for any analysis Survey 1 will be reduced in length to match Survey 2. This should not adversely affect the results, since most of the field measurements in the last 4 km of Survey 1 were green.

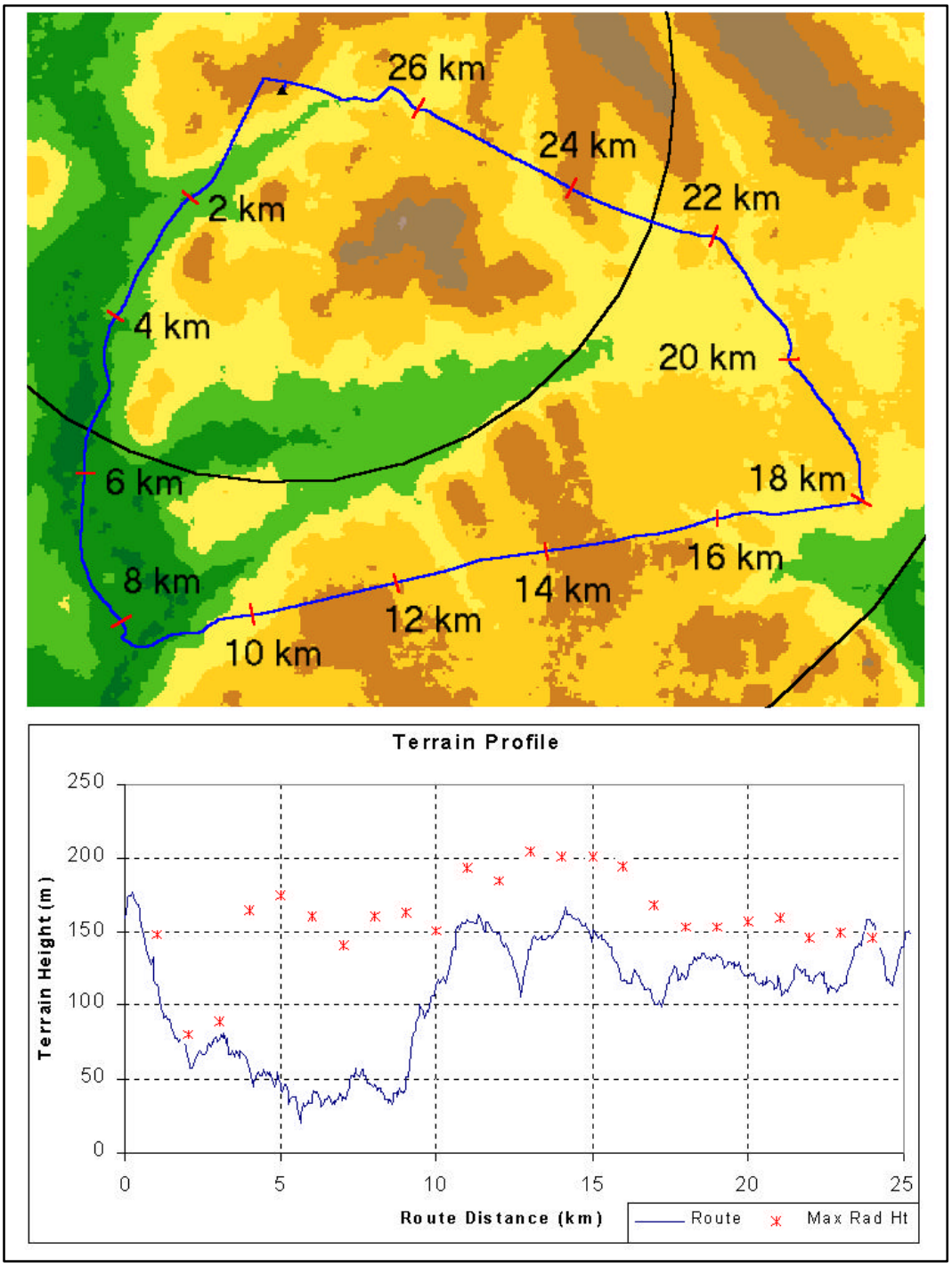

Figure 4-3: DTM of testing area and terrain profile along the test route. The profile includes maximum heights along radial profile from transmitter to 1 to 24 km marks.

4.1.2 Field Testing Results

The reference station was Headline Hill at an elevation of 135.8 m above sea level. The height of the transmitting antenna was 1.6 m above the terrain. The heights of the receiving antennas were 1.8 m above the terrain. The testing results for each receiver and survey overlay the terrain model in Figure 4-4. These results are described below.

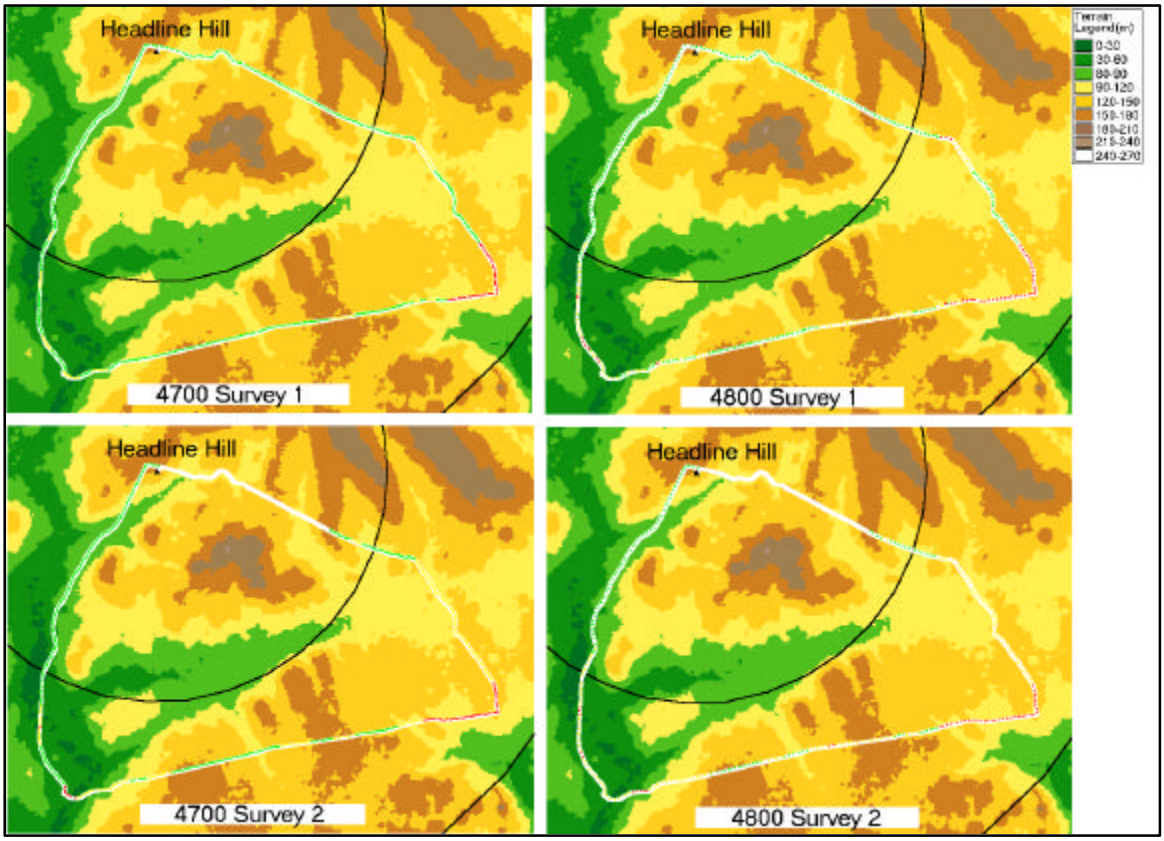

Figure 4-4: Results of Survey 1 and 2 overlaid DTM.

Survey 1-4700

The data link measurements for a majority of the first two legs were green with a few periods of yellow. The measurement became red for distance of 2 km at the junction of the second and third legs. For the remainder of the third leg, the majority of the measurements were green.

Survey 1-4800

The data link measurements were green for the first 5.5 km of the first leg. From this point on and past the junction of the first and second legs, the radio link was more variable having periods of green, yellow, and red. Similar to the 4700 near the end of the second leg, the radio link measurement became red for a 3 km stretch past the junction of the second and third legs. For the remainder of the third leg, the data link was green except for a short period where the signal became yellow and red.

Survey 2-4700

Similar to Survey 1, the majority of the data link measurements were green for the first and seconds legs. There were more periods of yellow measurements and two short periods of where the data link was not available. The data link was lost near the junction of the second and third legs for a distance of 2.5 km, similar to Survey 1. Once the data link was regained the measurements were yellow and then turned green closer to the reference station. For Survey 2, the measurements were stopped at approximately the 24 km mark.

Survey 2-4800

For the first 5 km of the first leg the data link measurement were green. From this point the data link was highly variable until the link was lost near the junction of the second and third legs. This time the data link was lost for 2.6 km. Once the data link was regained, similar to the 4700, the measurement was yellow until becoming green closer to the reference station.

Compared to the field measurements in survey 1, survey 2 had more yellow and red values. This trend is evident in both the 4700 and 4800 field measurements. Table 4-1 lists the percentage of the route that was green, yellow, red for each receiver and survey. There is 17% increase in yellow measurements for the 4800 with a corresponding 17% decrease in green. The 4700 had a 19% and 2% increase in yellow and red respectively, with a corresponding decrease of 21% in the green measurements. Based on the DTM the loss of the data link at the junction of legs 2 and 3, may be attributed to the large hill described earlier.

Table 4-1: Percentage green, yellow, and red measurements along the test route.

	4700			**4800**		
	Green	Yellow	Red	Green	Yellow	Red
Survey 1	76	14	10	53	30	17
Survey 2	55	33	12	36	47	17
Difference (2-1)	-21	19	2	-17	17	0

The test results from Survey 2 were different than what was expected. The signal was expected to be stronger due to the date of the survey and the fact that tree cover

would be less, therefore reducing attenuation. Nevertheless, the results were consistent between the two receivers and surveys.

4.2 Prediction Model Results

The models presented in Section 3.1.1 were employed with standard inputs to provide predictions of the test area. The results of these predictions are presented below.

4.2.1 Input Parameters

The input parameters for each software package were standardized and kept to readily available radio system parameters and digital terrain data. All radio system parameters were extracted from the RTK GPS radio base station manual [Trimble Navigation Limited, 1998a]. Table 4-2 lists the input and output parameters used for all propagation models. The transmitted power (effective radiated power-ERP) includes the amplifier power, cable loss, and transmitting antenna gain; calculations can be found in Appendix A. The antenna heights are relative to the local terrain as represented in the terrain model. The calculations of the received power were completed at a 30 m x 30 m grid sample resolution to match the Level 2 Digital Terrain Elevation Data (DTED) model. The output for each of the models was the received power in dBm in each 30 m x 30 m cell.

Table 4-2 Input Parameters and Values.

Input Parameters	Input Values
Transmitter	
Power (ERP):	40.82 Watts
Antenna Type:	Isotropic
Antenna Gain:	5 dBi
Antenna Height:	1.6 m
Polarization	Vertical
Receiver	
Antenna Gain:	
4700	5 dBi
4800	0 dBi
Antenna Height:	1.8 m
Model	
Sample Resolution:	30 m

4.2.2 Terrain Model Used

The DTM used for each model was a Digital Terrain Elevation Data (DTED) level 2 generated for the Department of National Defence using Synthetic Aperture Radar (SAR) interferometry (InSAR) using European Remotes Sensing (ERS) 1 and 2 sensors. The data used in the InSAR processing was collected on the 27th and 28th of April 1996. DTED level 2 has a grid spacing of 1 arc second (approximately 30 metres). The DTED specification calls for an absolute horizontal accuracy of less than 50 m and an absolute vertical accuracy of less than 30 m, both a 90% confidence level [DMA, 1996]. The final report [Atlantis, 2000] for the DTED generation stated that the terrain model meet both of these requirements.

Since the digital terrain model will provide the prediction models with information affecting the propagation of the radio waves, the DTED model was

compared to a more accurate terrain model to ensure that there are no major deficiencies. The DTED was compared to a digital terrain model of the test area generated in 1995 using aerial photography at a scale of 1:2,000 and vertical accuracy of 0.5 m at a 95% confidence level, referred to as “Base DTM”. For the test area the DTED has a mean height of 117.0 m with a standard deviation of 38.5 m compared to the Base DTM which has a mean height of 115.9 m with a standard deviation of 37.0 m. Three cross sections of the test area starting from the Headline Hill reference station were generated to compare the DTED to Base DTM. Figure 4.5 shows these comparisons.

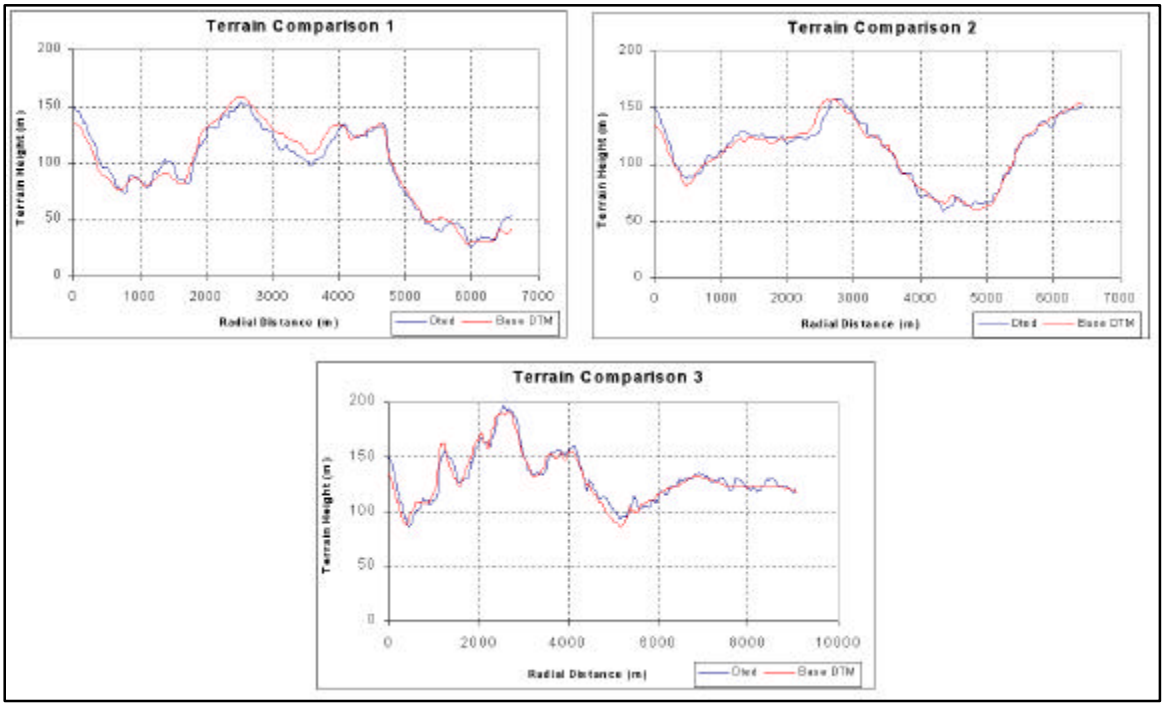

Figure 4-5: Terrain comparison plots.

The most significant difference between the two models the is height of the terrain at the location of the Headline Hill reference station. For the Base DTM the height is 134.6 m whereas the DTED is 150 m, compared to the GPS processed height of 135.8 m (All heights are above mean sea level). Since both WinProp and CRC-COV use the height of the antenna plus local terrain at the location of the transmitter, any error in height of the terrain model will be reflected in all prediction results.

4.2.3 Prediction Results

Using the parameters and terrain model described above each model was used to generate predictions of the average received power (dBm) throughout the test area. The results for the 4700 and 4800 predictions are illustrated in Figures 4-6 and 4-7. These figures also include concentric circles representing 5 and 10 km distances from the Headline Hill reference station. A standard legend for the predictions was chosen that ranges from light green to light red, where the highest value of the light red represents the sensitivity of the receiver. The only difference between the two sets of predictions is that the 4700 predictions take into account the 5 dBi receiver antenna gain.

The most evident difference between the predictions presented in Figures 4-6 and 4-7 is the pattern in the LR and OH (CRC) models. The concentric predictions indicate that the major influence on the prediction is the separation distance between the transmitter and receiver and not the terrain variations. The PE, TIREM, and Predict all show varying degrees of a weaker signal in the valley behind the large hill compared to the OH (WinProp) which indicates a stronger signal.

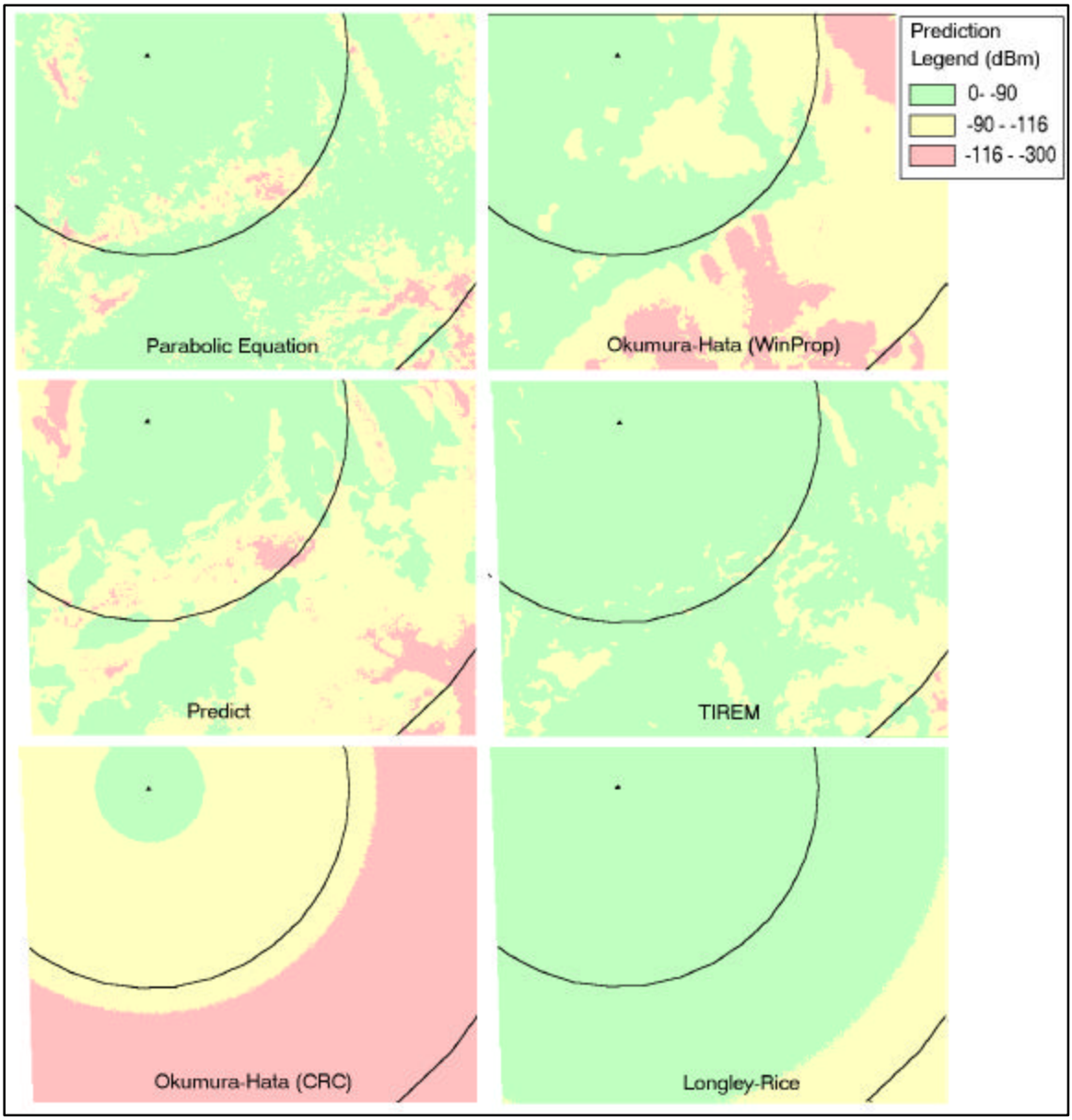

Figure 4-6: 4700 Prediction results.

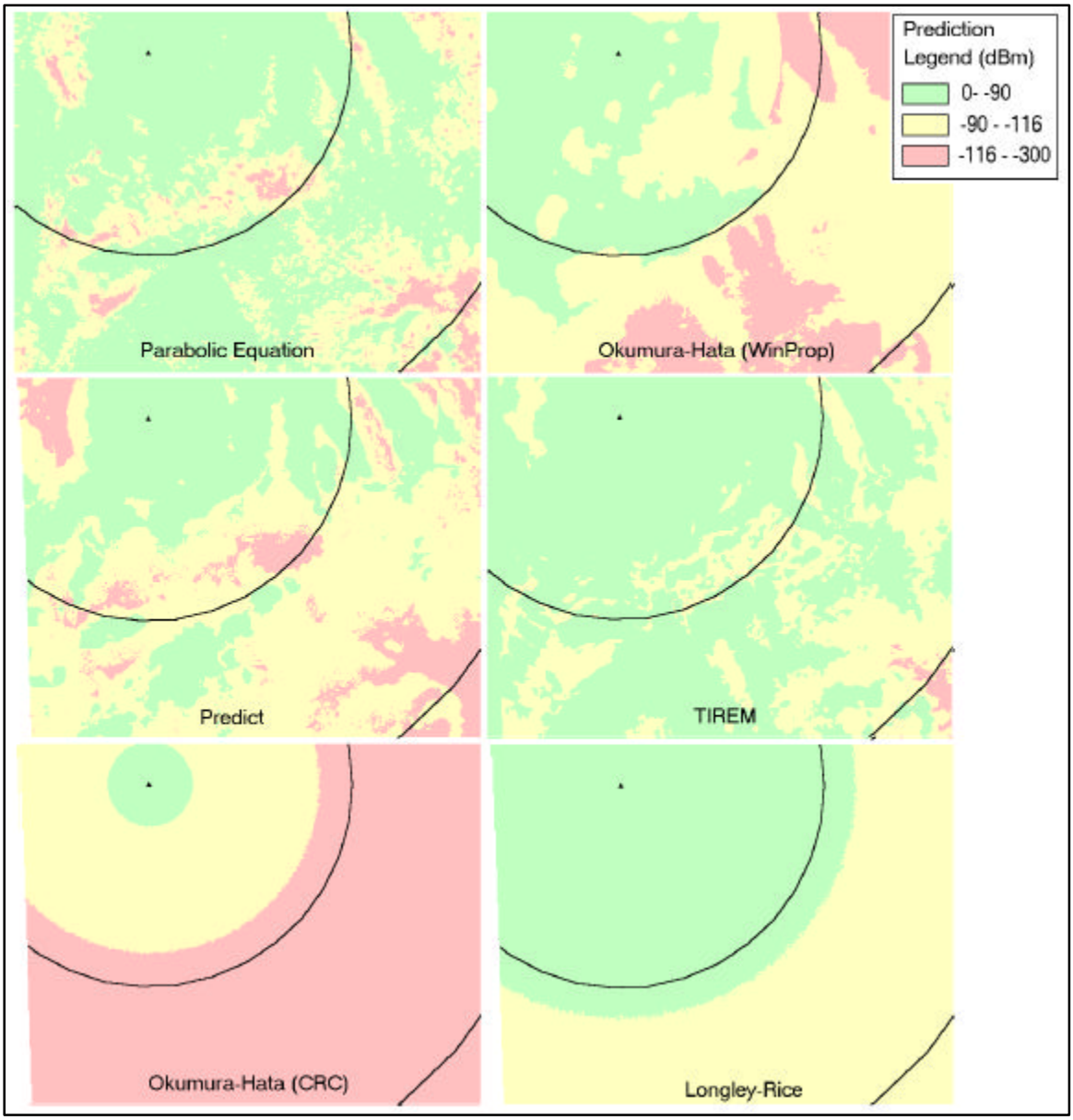

Figure 4-7: 4800 Prediction results.

4.3 Comparison and Analysis

The comparison criteria described in Section 3.3 will be used to determine which model or models had the best performance compared to the field measurements. Each model will be presented using the three criteria. The figures in the following section contain the field measurements overlaying the predictions. The figures also include the corresponding plot of the route field measurements and predicted received power (dBm) against distance along the route (km). The fixed values of -64 dBm, -90 dBm, and -116 dBm were chosen for the field measurements of green, yellow, and red respectively to match the maximum values of yellow and red in the prediction results colour legend.

For the coverage probability comparison the predicted average received power was extracted for each field measurement and receiver. The sensitivity of the 4700 and 4800 receivers is -116 dBm (12 dB SINAD). The standard deviation of 12 dB was used. This was determined using the recommendations found in Section 2.3.3.4 and the calculations can be found in Appendix B. A coverage probability of 95% was chosen for this comparison. Table 4-3 lists the proposed statistical test for each field measurement and respective prediction.

Table 4-3: Statistical test for each field measurement and corresponding prediction.

Field Measurement	Test
Green	Probability (Prediction > Sensitivity) > Coverage Probability
Yellow	Probability (Prediction > Sensitivity) > Coverage Probability
Red	Probability (Prediction > Sensitivity) < Coverage Probability

For example, if a field measurement is green and if the probability of the prediction greater than the sensitivity is larger than coverage probability then the test passes and fails otherwise. For each prediction and field measurement combination the test will either pass or fail. Further analysis will only present the percentage of correct predictions (passes) or acceptance of the test.

Based on the field measurement technique and proposed tests in Table 4-3, an ideal prediction model should have a high percentage of correct predictions for both the green and red measurements. For this project a yellow measurement is an indication of a weaker signal, but RTK positioning is still possible (Fixed or Float). Using this measurement technique and Table 4-3, an ideal model should have a relatively high number of correct predictions, but not as great as the green.

4.3.1 Parabolic Equation

Figures 4-8 and 4-9 show the field test results from the 4700 and 4800 for Survey 1 and 2 and the PE predictions. The plots of the predicted received power and test results along the route show a high degree of correlation for each survey. The variations in the measurements between 5 to 10 km and 14 to 19 km marks correspond with those of the lower predicted values. For both surveys and receivers, the green measurements correspond to higher predicted values and the red measurements correspond to the lower predicted values.

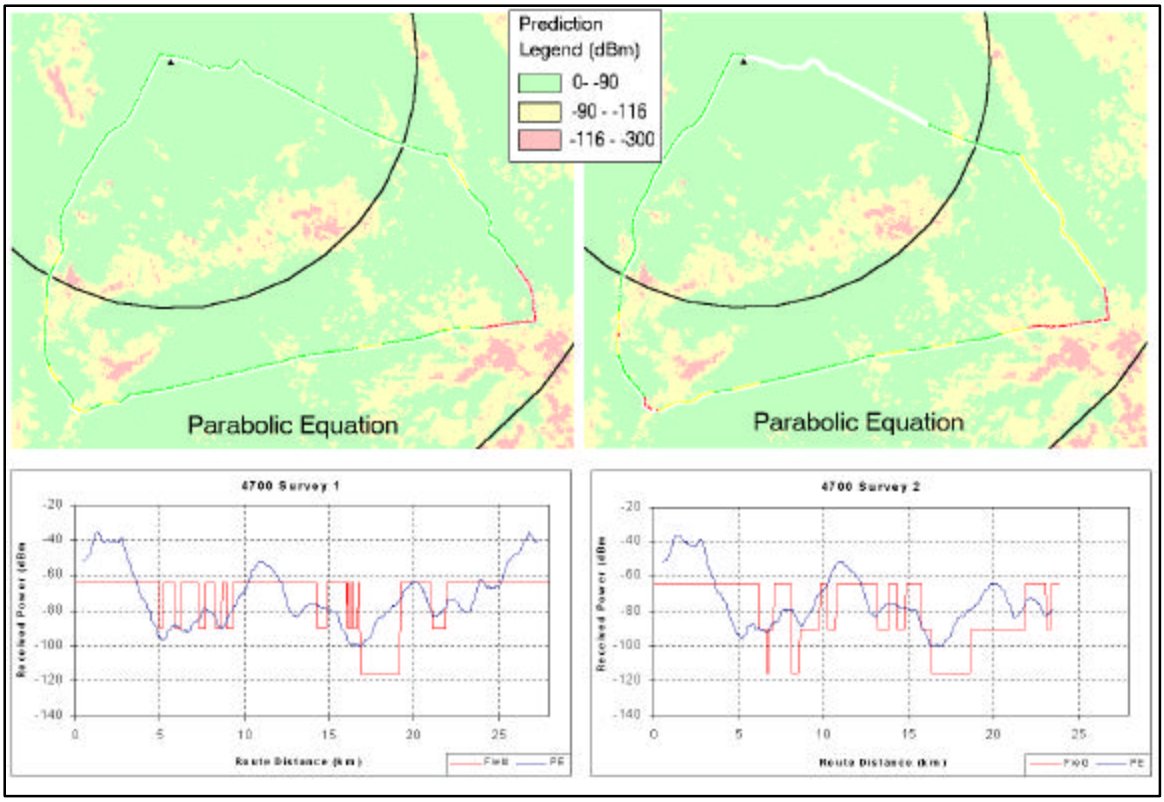

Figure 4-8: 4700 Survey 1 and 2 results and PE prediction results.

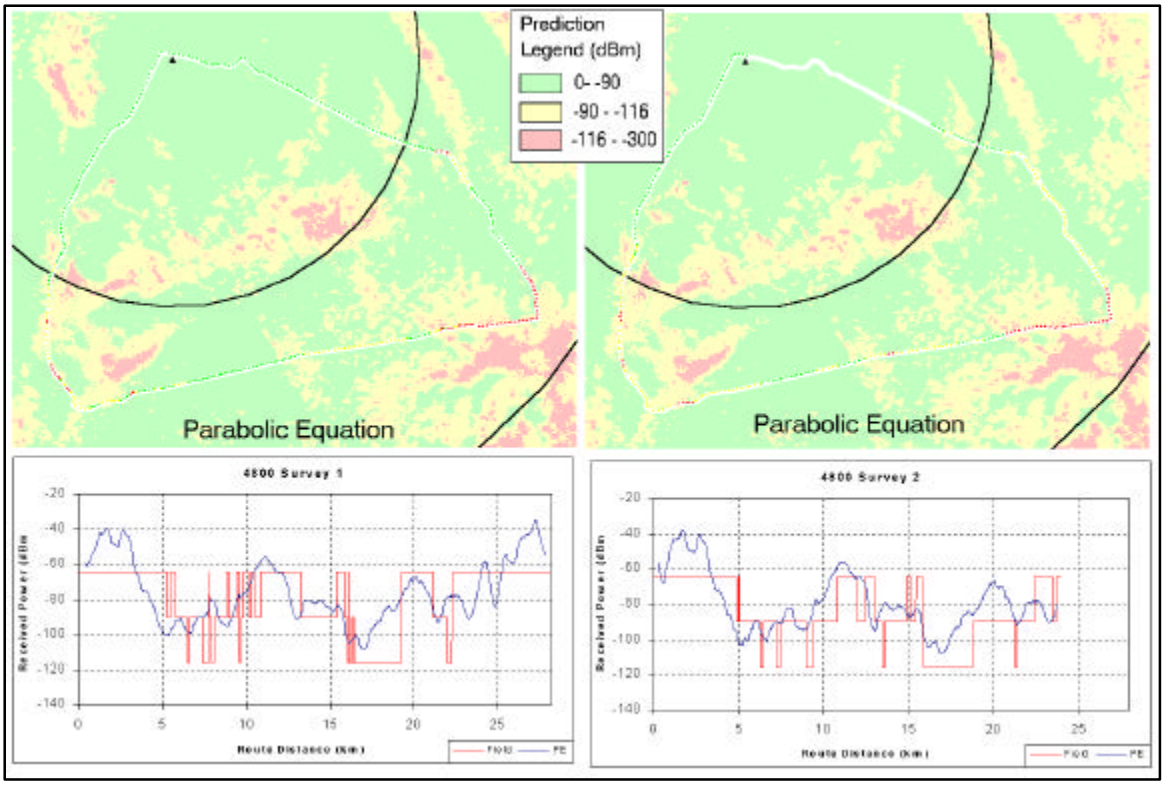

Figure 4-9: 4800 Survey 1 and 2 results and PE prediction results.

Table 4-4 lists the percentage of acceptance for the PE predictions. The green measurements show the highest percent of correct predictions followed by yellow. The percentage of correct red predictions is quite low for both 4700 and 4800 receivers in each Survey. The green predictions are the most consistent for both receivers and surveys, whereas the red and yellow show a variation between 3 and 13 percent. The high percentage of green and low percentage of red may indicate an overly optimistic prediction.

Table 4-4: Percentage of correct predictions for PE.

	4700			4800		
	Green	Yellow	Red	Green	Yellow	Red
Survey 1	93.2	81.0	19.1	92.1	83.8	36.5
Survey 2	96.6	93.9	32.1	93.0	87.2	44.4
Average	94.9	87.5	25.6	92.5	85.5	40.4

4.3.2 Predict

Figures 4-10 and 4-11 show the field test results from the 4700 and 4800 for Survey 1 and 2 and the Predict predictions. The plots of the received power and test results along the route show a high degree of correlation for each survey. The variations in the measured signal strength between 5 to 10 km and 14 to 19 km marks correspond with lower predicted values. The green measurements for the 4700 and 4800 in both surveys correspond to the higher predicted values, whereas the red values correspond well to the lower predictions.

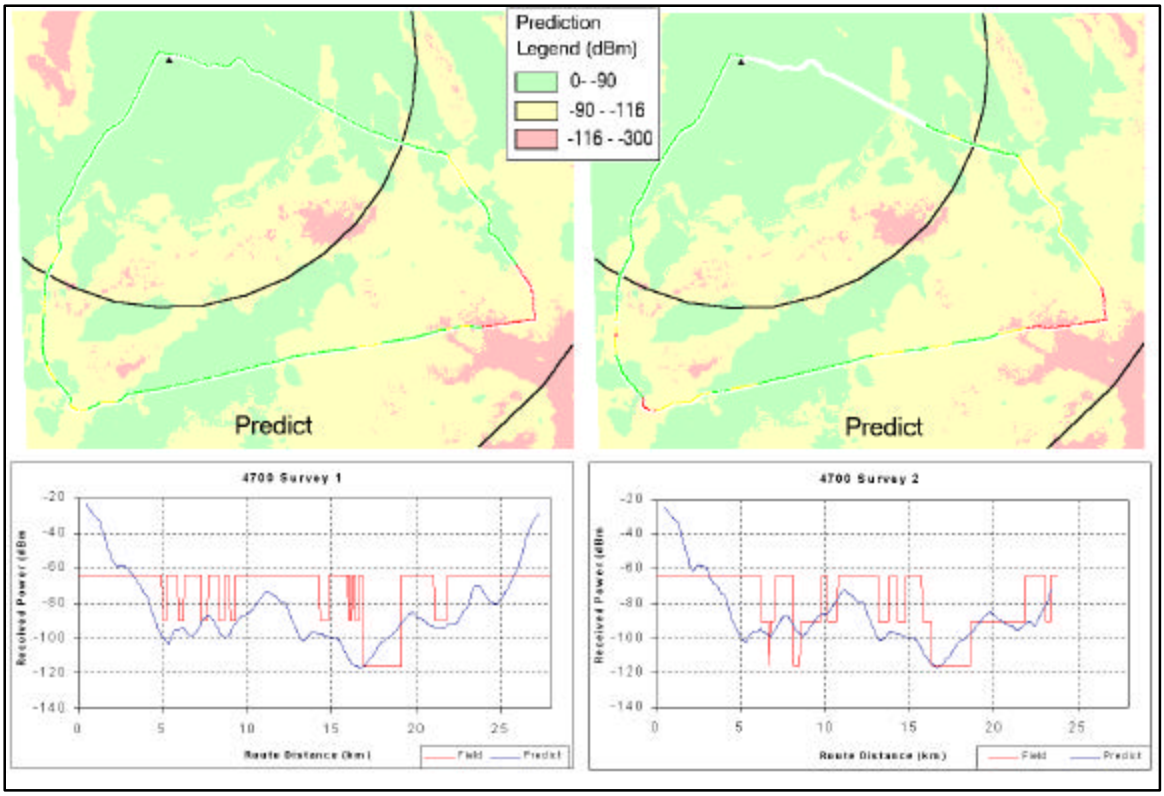

Figure 4-10: 4700 Survey 1 and 2 results and Predict prediction results.

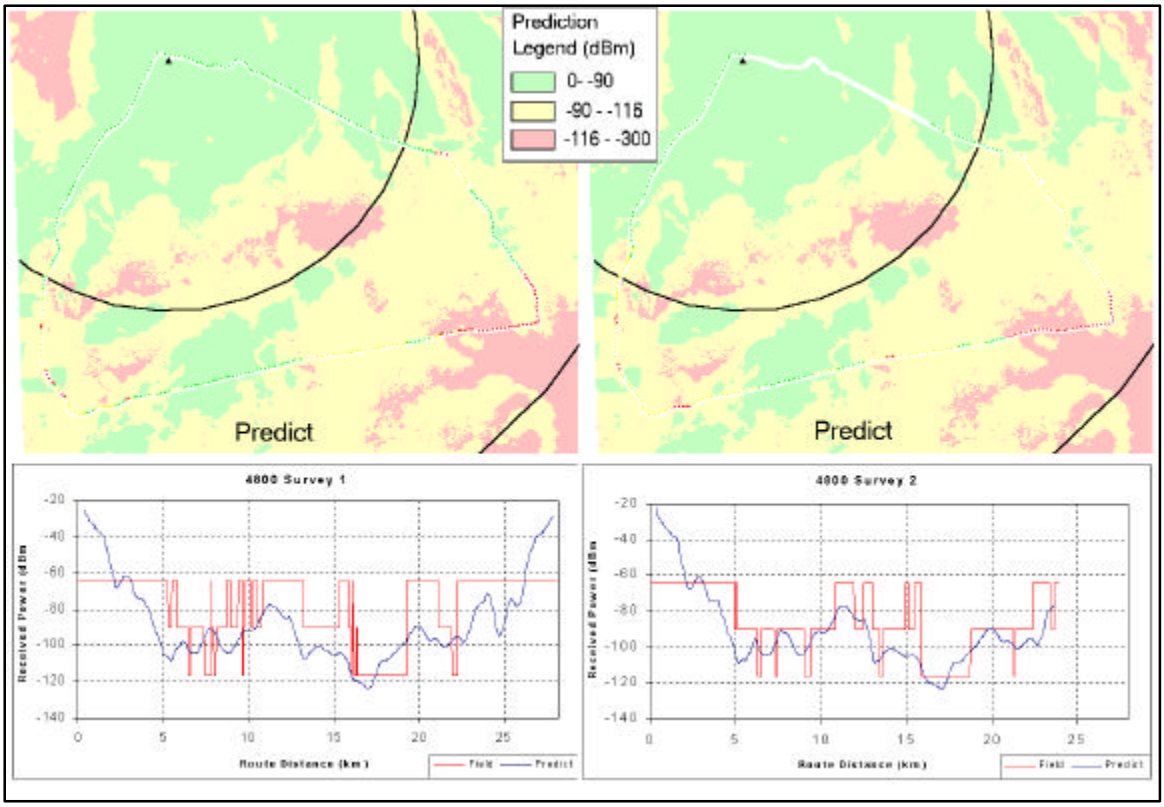

Figure 4-11: 4800 Survey 1 and 2 results and Predict prediction results.

Table 4-5 contains the percentage of acceptance for both receivers and surveys. Overall the red measurements were predicted correct for both receivers and surveys. The percentage of correct green predictions is consistent for both receivers and surveys, whereas the red and yellow had variation between 10 and 23 percent.

Table 4-5: Percentage of correct predictions for Predict.

	4700			**4800**		
	Green	Yellow	Red	Green	Yellow	Red
Survey 1	72.7	44.3	81.0	76.7	21.5	82.5
Survey 2	80.0	60.6	91.1	81.4	44.5	95.9
Average	76.3	52.4	86.1	79.0	33.0	89.2

4.3.3 TIREM

Figures 4-12 and 4-13 show the field test results from the 4700 and 4800 for Survey 1 and 2 and the TIREM predictions. The plots of the predicted received power and test results along the route show a high degree of correlation for each survey. The variations in the measured signal strength between 5 to 10 km and 14 to 19 km marks correspond with lower predicted values. The green measurements for both receivers and surveys correspond well to the higher predictions and the red measurements correspond well to the lower predictions.

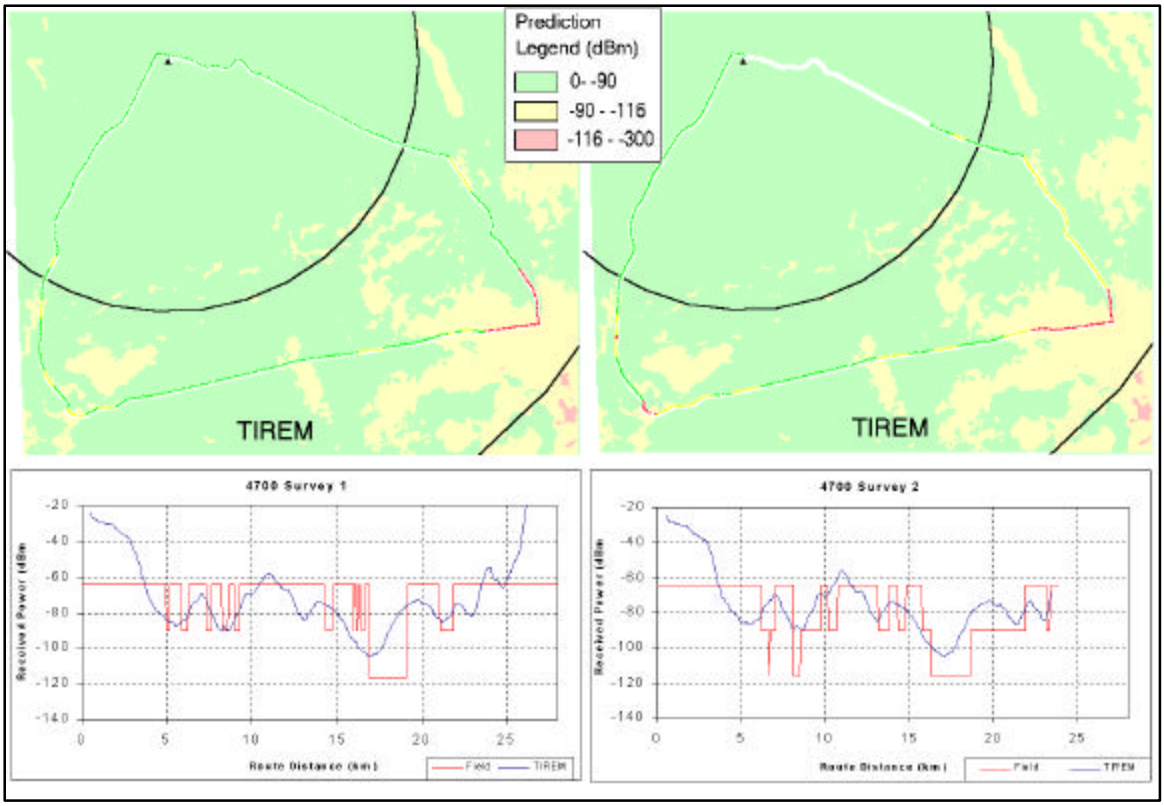

Figure 4-12: 4700 Survey 1 and 2 results and TIREM prediction results.

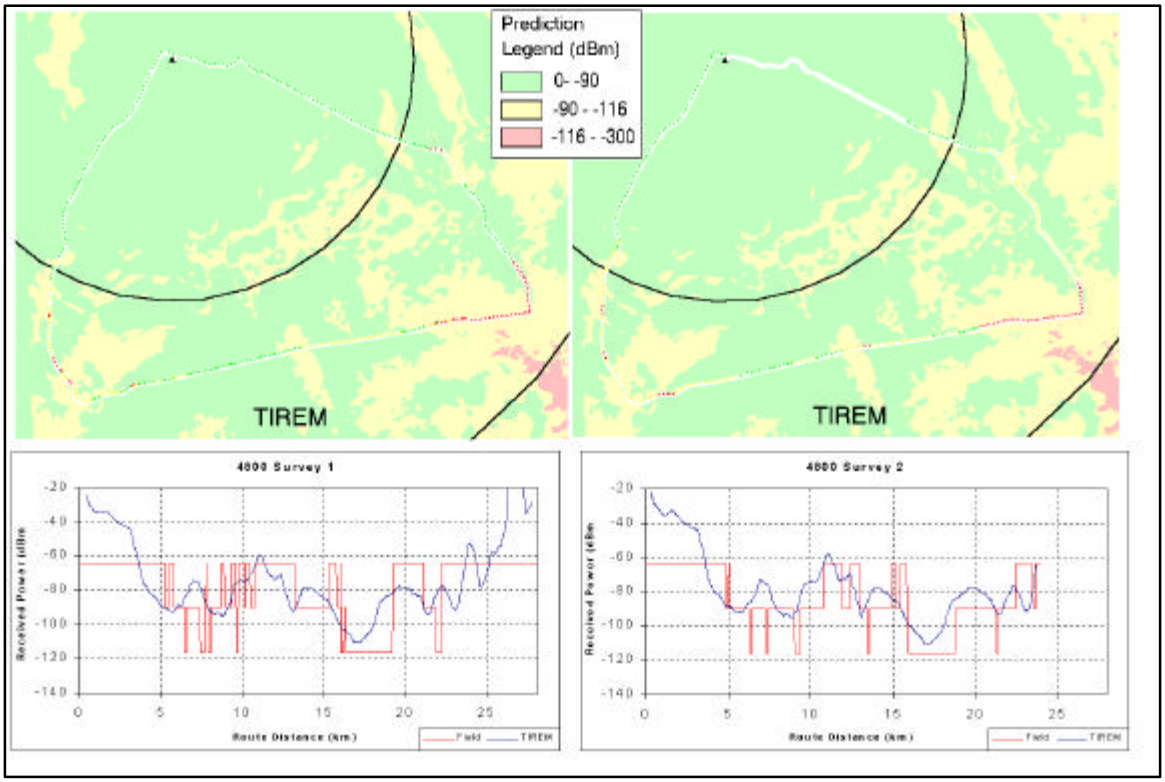

Figure 4-13: 4800 Survey 1 and 2 results and TIREM prediction results.

Table 4-6 lists the percentage of test acceptance for the TIREM model. The percentage of correct green predictions is very high, as is the yellow. The correct red predictions are mid range. Overall the correct predictions increase from Survey 1 to 2. Like the PE, the TIREM model may be considered optimistic.

Table 4-6: Percentage of correct predictions for TIREM.

	4700			**4800**		
	Green	Yellow	Red	Green	Yellow	Red
Survey 1	97.1	83.5	52.4	97.7	85.5	50.7
Survey 2	100	95.6	58.9	96.5	95.3	62.8
Average	98.6	89.6	55.7	97.1	90.4	56.7

4.3.4 Okumura-Hata (CRC)

Figures 4-14 and 4-15 show the field test results for the 4700 and 4800 for Survey 1 and 2 and the OH (CRC) predictions. The predicted received power shows a slight increase (≈5 dBm) between the 10 and 15 km marks (along the route) as the receivers are closer to the transmitter. The plot of predicted received power and field tests along the route show no correlation for either receivers or surveys.

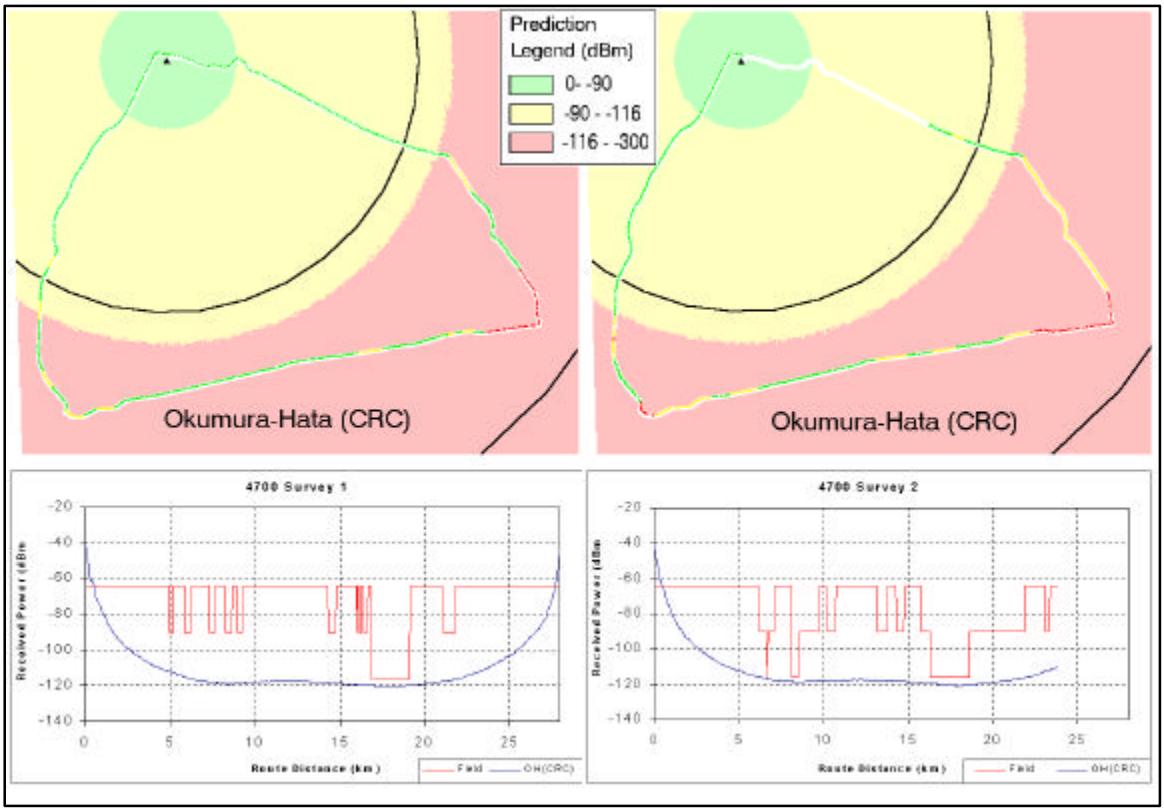

Figure 4-14: 4700 Survey 1 and 2 results and OH (CRC) prediction results.

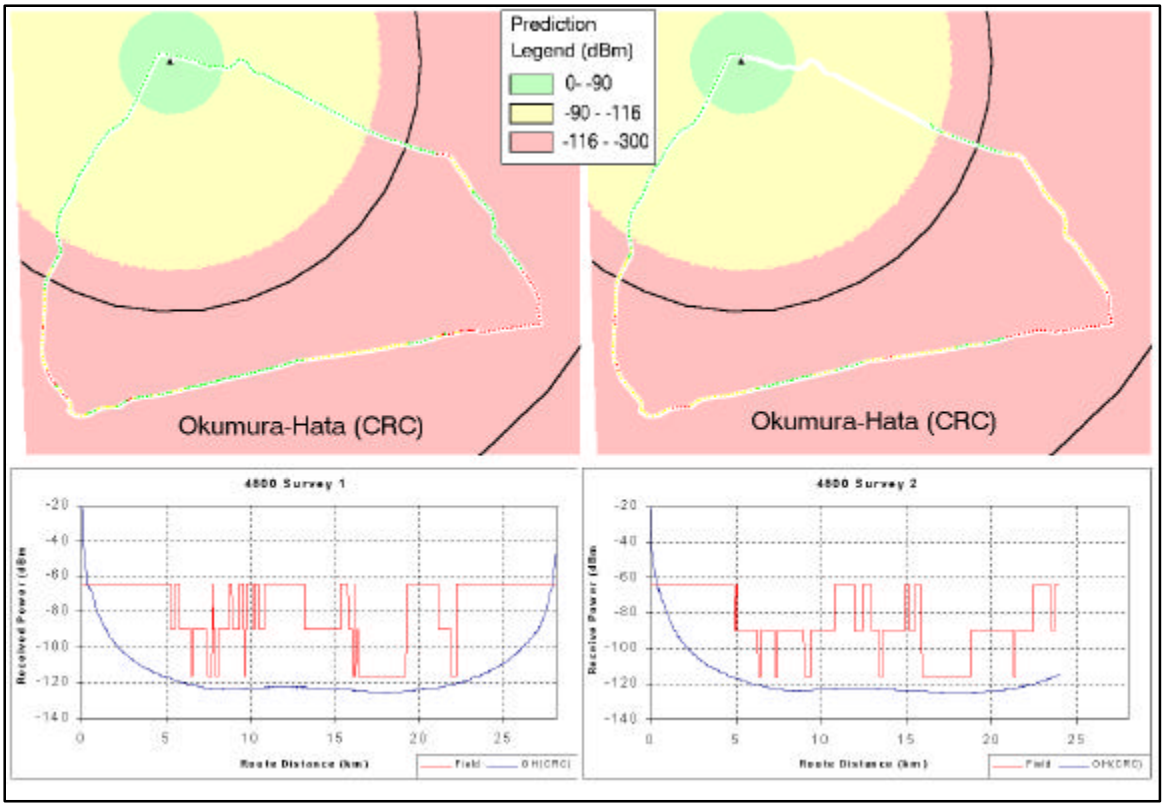

Figure 4-15: 4800 Survey 1 and 2 results and OH (CRC) prediction results.

Table 4-7 lists the percentage of acceptance for the OH (CRC) model. The correct red predictions are 100 percent for all receivers and surveys. The green and yellow is very low for both receivers and surveys. As with the visual comparison and route analysis the coverage probability comparison shows very little correlation.

Table 4-7: Percentage of correct predictions for OH (CRC).

	4700			**4800**		
	Green	Yellow	Red	Green	Yellow	Red
Survey 1	11.7	0	100	12.5	0	100
Survey 2	15.9	0	100	21.2	0	100
Average	13.8	0	100	16.8	0	100

4.3.5 Okumura-Hata (WinProp)

Figures 4-16 and 4-17 show the field test results for 4700 and 4800 for Survey 1 and 2 and the OH (WinProp) predictions. The plan view plots of the field test and predictions reveal that the WinProp implementation of the OH does not just rely on distance between transmitter and receiver. The plot of the test results and the predicted received power show very little correlation for either receivers or surveys.

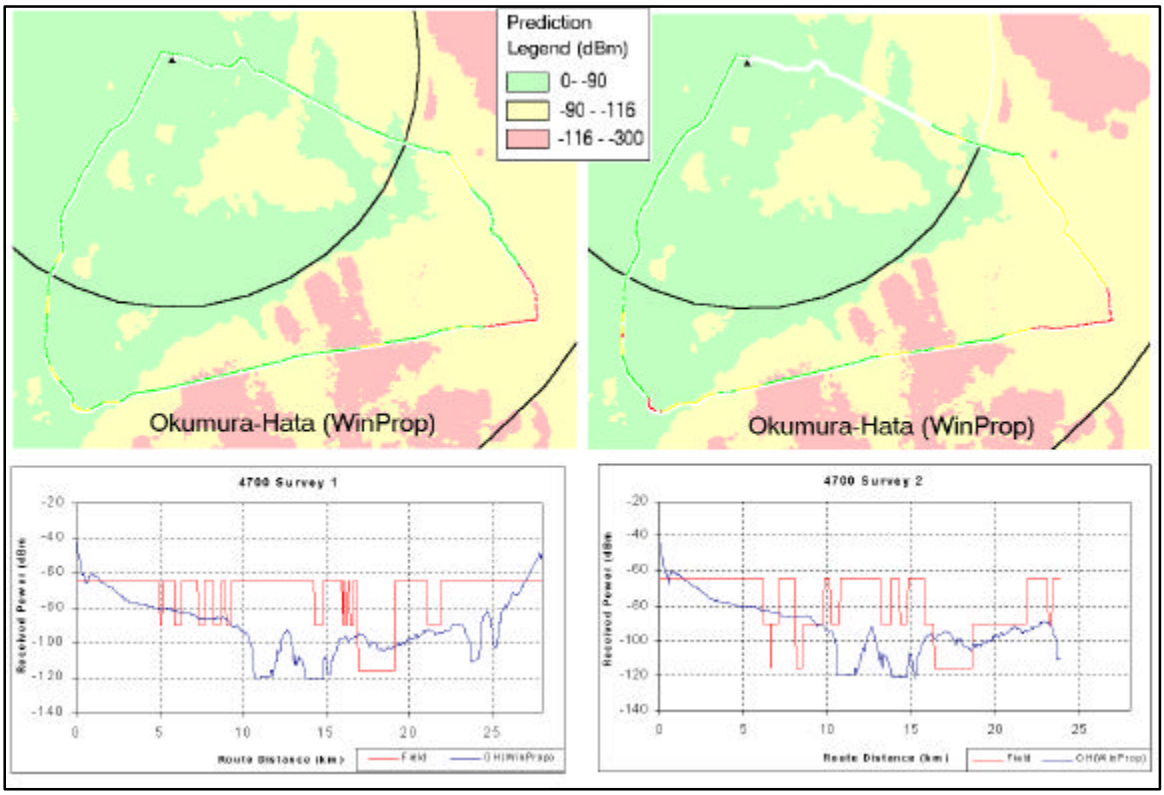

Figure 4-16: 4700 Survey 1 and 2 results and OH (WinProp) prediction results.

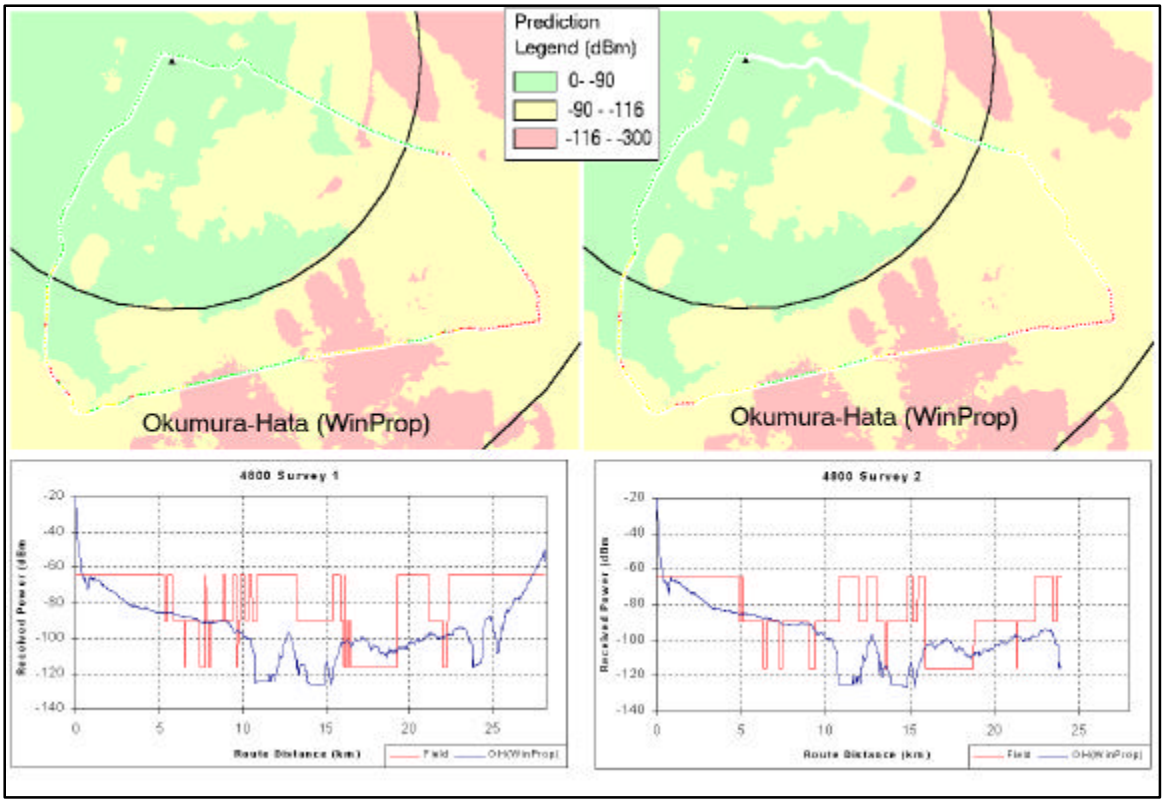

Figure 4-17: 4800 Survey 1 and 2 results and OH (WinProp) prediction results.

Table 4-8 lists the percentage acceptance for the OH (WinProp) model. The correct red predictions are the greatest overall. The yellow and red predictions decrease from Survey 1 to 2 and have a variation of 6 to 25 percent.

Table 4-8: Percentage of correct predictions for OH (WinProp)

	4700			**4800**		
	Green	Yellow	Red	Green	Yellow	Red
Survey 1	61.7	76.0	81.0	47.8	44.6	86.3
Survey 2	69.8	50.6	62.5	65.3	37.8	79.6
Average	65.77	63.3	71.7	56.6	41.2	82.9

4.3.6 Longley-Rice

Figures 4-18 and 4-19 shows the field test results for the 4700 and 4800 for Survey 1 and 2 and the LR predictions. The predicted received power shows very little variation beyond 5 km from the transmitter along the route. The plot of predicted field strength and field tests along the route show no correlation for either receivers or surveys.

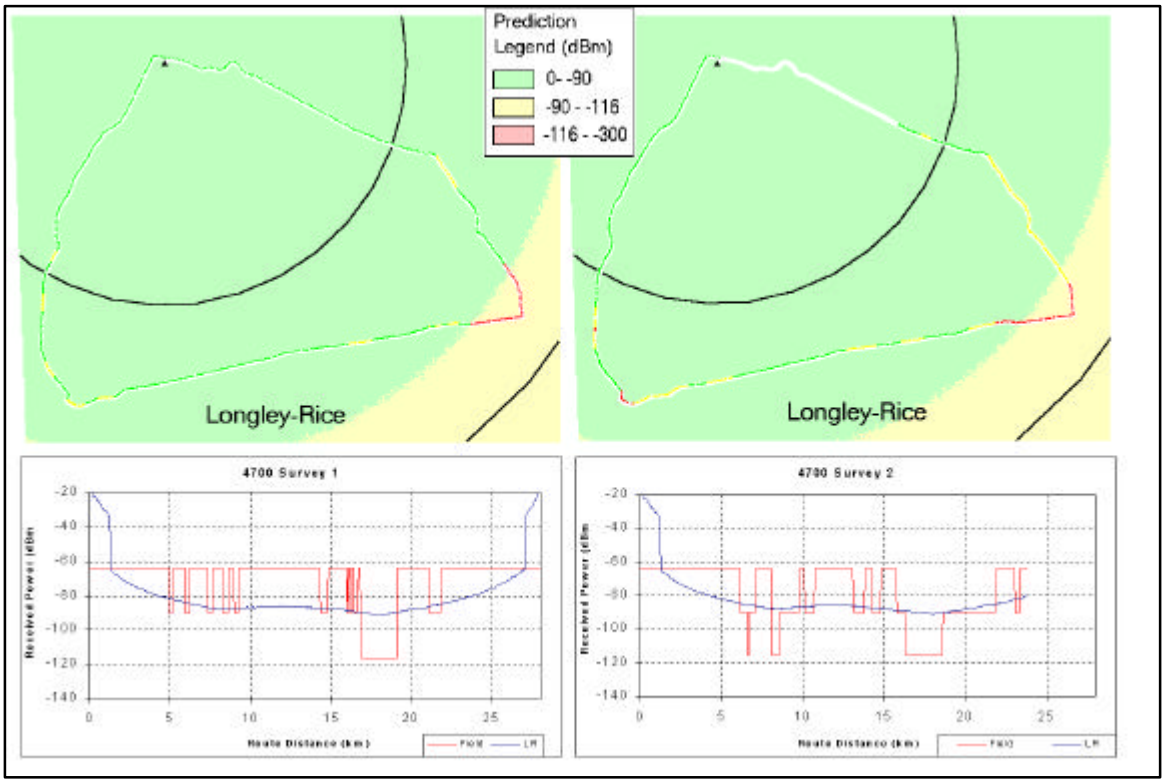

Figure 4-18: 4700 Survey 1 and 2 results LR prediction results.

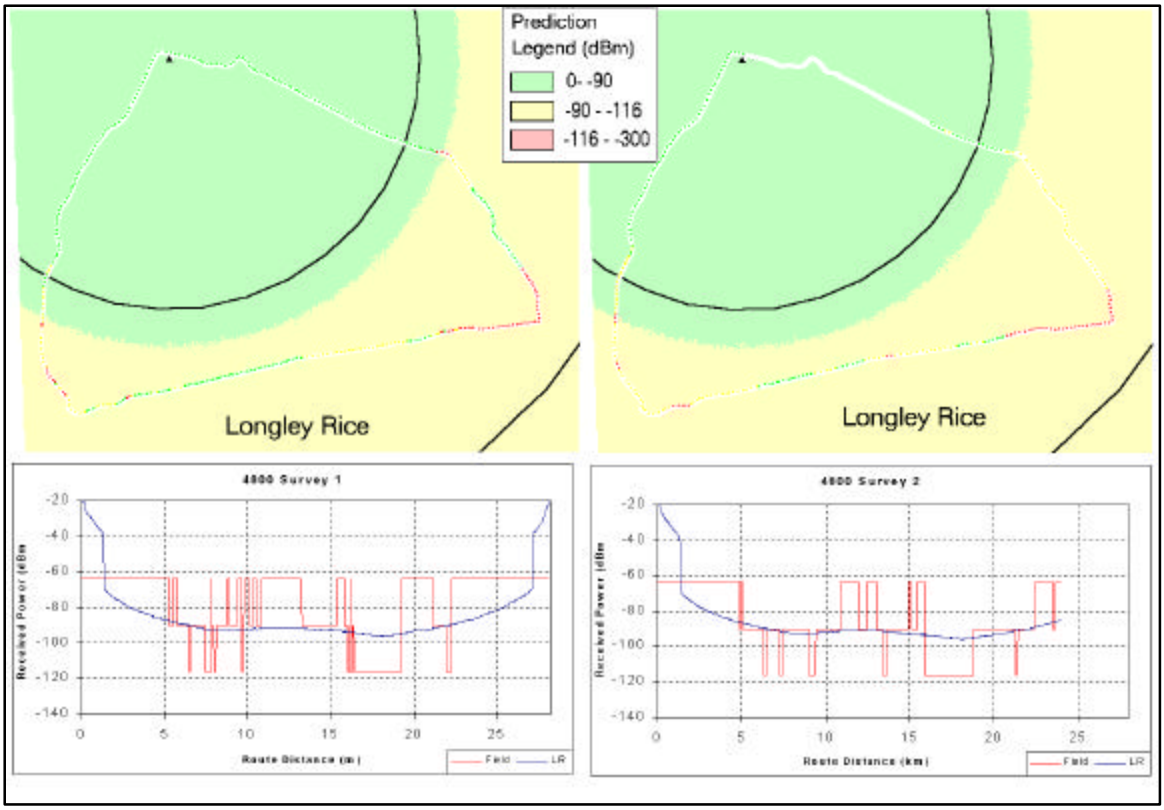

Figure 4-19: 4800 Survey 1 and 2 results and LR prediction results.

Table 4-9 lists percentage of true hypotheses for the LR predictions. The green and yellow are 100 percent for both receivers and surveys, whereas the red has 0 percent. Like the visual comparison and the route analysis, the coverage probability comparison shows very little correlation.

Table 4-9: Percentage of correct predictions for LR.

	4700			**4800**		
	Green	Yellow	Red	Green	Yellow	Red
Survey 1	100	100	0	100	100	0
Survey 2	100	100	0	100	100	0
Average	100	100	0	100	100	0

4.3.7 Model Inter-comparison

Based on the analysis of the results presented in the previous section it is evident that some of the models do not perform very well in the given circumstances. The visual comparison, route analysis, and percentage of true hypotheses show that the Predict, TIREM, and PE perform the best overall in these given circumstances. These three models will be discussed and compared further.

The plots showing the predicted received power along the test route of the Predict, TIREM, and PE have very similar trends in the peaks, valleys, and slopes. Figure 4-20 shows all three of these models plotted together. Other than the minor difference between 5 and 10 km marks, all models follow the same trends.

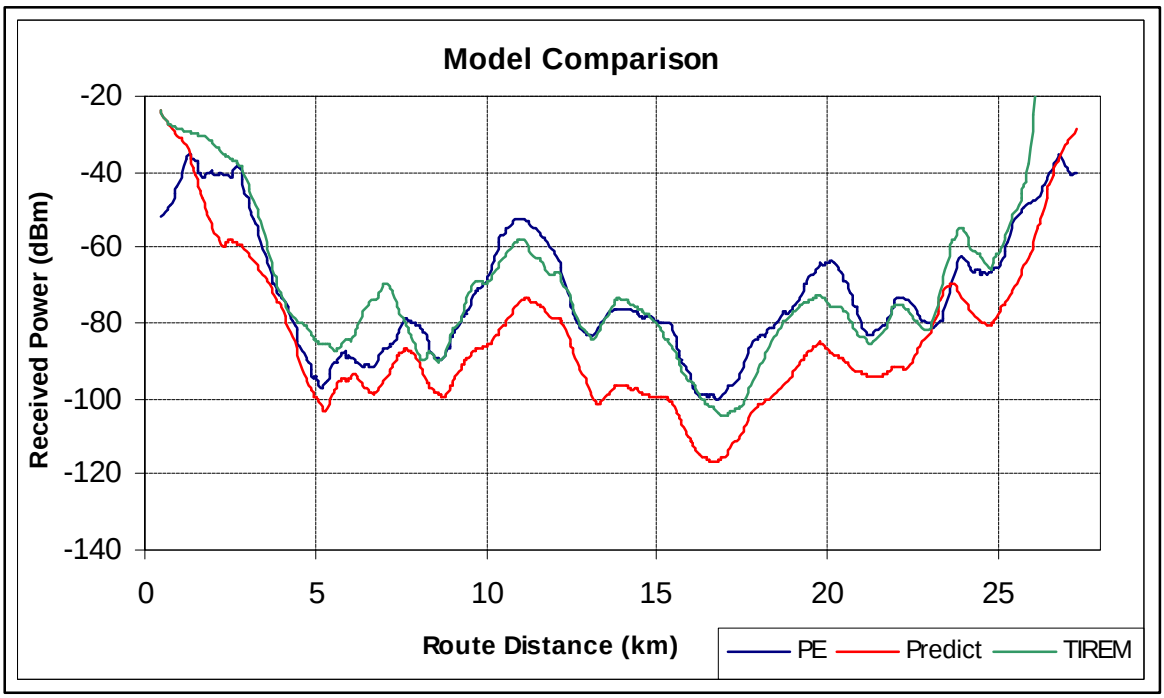

Figure 4-20: Predicted received power of PE, Predict, and TIREM models along test route.

Overall the TIREM and PE models are closer in scale along the entire route. The Predict results are lower than both the PE and TIREM, with differences up to 20 dBm between the 5 and 25 km marks. This difference accounts for the greater number of correct red predictions determined by the Predict model, when compared to the PE and TIREM. The PE and TIREM may be classified as “optimistic”, whereas Predict may be classified as “pessimistic”.

As expected, there is not a perfect model that predicts the coverage and no coverage exactly and is evident from the results presented in the previous sections. From an RTK GPS user point of view the most important factor related to the data link is where there is no coverage or the potential for problems with the coverage. Therefore, based on the highest percentage of correct predictions for the red measurements, the Predict model performs the best followed by the TIREM then the PE.

4.3.8 Potential Error Sources

The results show that the models do not predict the data link coverage perfectly. In the comparison there are potential error sources that may affect the results. The following will present potential error sources from this project and their potential effect on the results.

4.3.8.1 Field Measurements

The type of field measurement used in the testing was very coarse, either there was a signal (green or yellow) or there was no signal (red). Any blunders in the measuring of signal were minimized by using the same person to make measurements in

both surveys. A different measurement technique that looks at the actual signal strength and data being received could be investigated to refine the measurement, but would require more processing and different equipment than that used in this project.

4.3.8.2 Predictions

In this project the major inputs for the models were: DTM, antenna pattern, transmitting power, and height of transmitting and receiving antennas. As illustrated in Section 4.2.2, the DTM used in this project had error at the location of the transmitting antenna and variations throughout the model when compared to the Base DTM. The DTED was used in both software packages and for all models, therefore, any errors in the DTM should be reflected in all predictions. This error caused by the DTM for each model is not known and can not be qualified without further study.

The inputs in the prediction models, other than the DTMs, were kept to readily attainable radio system characteristics. The transmitting power used for the prediction model was based on the documented base station transmitting power, cable losses, and transmitting antenna gain. The actual field setup tried to replicate these conditions, but the actual transmitting power may be different. The type of transmitting antenna pattern used was isotopic, which is a hypothetical, lossless antenna having equal gain in all directions. The actual transmitting antenna has a specific pattern other than isotropic. In consultation with the representatives from the respective communication planning software developers, it was stated that the effect should be minimal. The effect of the antenna pattern is beyond the scope of this project and would require further study and is not in line with the goal of keeping the inputs relatively simple.

The effect due to land cover on the predictions was not investigated in this project. The area between the transmitter and test route was composed of various type of vegetation of varying heights. Yacoub [1993] states the attenuation due to trees is complex due to the number of variables involved. These variables include: height, shape, density, season, humidity, and polarization. Since the vegetation was not taken into account, further study would be required to quantify the error due to neglecting the effect.

4.3.8.3 Other Factors

This project employed the use of two different communications software packages. Each package has its respective input and output data format. For example, CRC-COV uses DTED as a direct input, whereas WinProp requires the DTM to be in a proprietary format. ArcView was used as a common platform to compare and manipulate data. Appendix C lists the flow of the data for each software package to manipulate the results into ArcView Grid format. The data for each step was verified throughout the process to minimize any error and the effect on the results. It is estimated that the greatest error may be a shift in the prediction result of up to one grid square (30 metres).

4.4 Implementation Considerations

The ultimate goal of this project is to recommend a prediction model to be implemented into an RTK GPS planning tool. As shown in Section 4.3, the results of the comparisons were very close between the PE, TIREM, and Predict models. Therefore, the decision on which model to be implemented is based on the availability of current documentation and source code must be considered.

Based on the research for this project, the PE model has the most extensive and accessible documentation, specifically a recently published text by Dr. Levy [Levy, 2000] that provides an extensive reference list and algorithms for implementing the PE in various circumstances. In discussions with CRC personnel with respect to implementing the Predict model, it was stated that implementation may be difficult due to the accessibility of the documentation. The research on the TIREM model found that both the original documentation and program is available, but was not located for this project [IEEE, 1998].

In the prediction process, the respective algorithms take into account detailed terrain paths between transmitter and receiver. This type of analysis provides a more accurate and realistic prediction, but affects the processing time. In practice, the prediction resolution should not be smaller than the grid spacing of the input DTM. As the prediction resolution the processing time increases, but the accuracy of the prediction may reach a limit. Any model implemented must optimize the processing time while maintaining required accuracy. This will require further investigation of the effect on accuracy and processing time.

5

CONCLUSIONS AND RECOMMENDATIONS

This chapter summarizes the material presented in this report and the results of this investigation. Section 5.1 reviews the principal and secondary goals of this study. Section 5.2 will summarize the results and the recommendations based on the results. Possible topics and areas of further research will be discussed in Section 5.3, with concluding remarks in Section 5.4.

5.1 Review of Research Goals

The principal goal of this research was to determine the best wave propagation model for rural areas to be used in a mission planning tool for RTK GPS surveying. In order to accomplish this several secondary tasks were carried out. These include:

1. *Research wave propagation models being used in the current communications planning software.* Five different models were chosen and are briefly described in Chapter 4.

2. *Develop a field testing method to validate the models chosen.* The proposed testing method is described in Chapter 3. The results of the testing method are presented in Chapter 4 along with recommendations for future measurements.

3. *Present criteria to compare the prediction results and the field measurements.* The criteria are proposed in Chapter 3 and then used in Chapter 4 to compare the predictions to the field testing

4. *Make a recommendation of the best model to be implemented in a mission planning tool for RTK GPS surveying.* The recommendation is based on the comparison criteria and implementation considerations and can be found in Chapter 4.

5.2 Summary of Results

The field test and model prediction results and the respective comparisons can be found in Chapter 4. A description of the comparison criteria can be found in Chapter 3. The criterion included a visual comparison, route profile analysis, and coverage probability comparison.

It was evident from the visual comparison that the predictions of the OH (CRC) and LR models were more dependent on T-R separation then terrain information. Whereas the PE, TIREM, and Predict all consider terrain information in the predictions. All three models showed a weaker received power, to some degree, in the valley discussed in Section 4.1.1, as would be expected. On the other hand, the OH (WinProp) predicted an increase in the signal strength in the valley. The models that performed the best in the visual comparison were PE, TIREM, and Predict.

The route analysis looked at the plot of predicted received power and measured signal strength along the test route. The field measurement consisted of having a signal or not having a signal, therefore a direct comparison of the actual received power and predicted received power was not possible. Instead the trends of the two were analyzed. Similar to the visual comparison, the PE, TIREM, and Predict models perform the best in the given conditions and show a high correlation between the prediction and field measurements. The OH (CRC), OH (WinProp), and LR show very little correlation between the two. Section 4.3.7 shows that the predictions of the PE, TIREM, and Predict show similar trends along the test route, the major difference being the scale difference of the Predict model.

The coverage probability allows for a statistical test between the field measurement and the prediction to be carried out. For the coverage probability of 95% and a standard deviation of 12 dB, the PE, TIREM, and Predict performed the best overall. As discussed, from the point-of-view of a RTK GPS user, the areas where there is no data link coverage are of most interest. Based on the model inputs (DTM) and the given circumstances, the Predict model had the highest percentage of correct red predictions, of the three, for both surveys and receivers.

Based on the criteria, the PE, TIREM, and Predict perform the best in the given conditions. Without considering the effects on the predictions due to land cover, the best model from the RTK GPS user point-of-view is the Predict.

Implementation of any of the three models into a mission planning tool will require documentation and references explaining the details. Based on the research for this project it is apparent that the PE has the most documentation outlining various

implementation methods and in particular the newly published text by Levy [Levy, 2000]. The Predict model performed the best in the project. However, based on conversations with CRC personnel, an independent implementation of the Predict model may be difficult given the readily available documentation. Although not investigated in this project, IEEE [1988] suggests that the TIREM computer program is available with all documentation. From an implementation point-of-view, the PE and TIREM models are recommended. Further research into the effect of land cover should also be investigated to "fine tune" any implementation.

5.3 Suggestions for Further Research

This investigation has looked at various complex wave propagation models and their possible use in an RTK GPS mission planning tool. With the increase in mobile communications, the prediction planning software and input information, such as accurate DTM and land cover information, are attracting more research interest. Based on the research and work completed in this project the following recommendations for further research are made:

Implement the recommended models. The PE or TIREM model could be either implemented into a stand-alone software program or a module for a GIS, like ArcView. As part of the implementation, the effect of prediction resolution and DTM accuracy should also be investigated. Other inputs such as antenna patterns

and land cover to “fine tune” the prediction could also be investigated and implemented based on the findings.

Improved field measurement technique. The field measurement technique was kept simple on purpose, but provided coarse results that limited the comparison to the predictions. Further investigation into an improved field measurement technique should be completed. One option may be to look at the data being transmitted and received and the actual RTK processing being carried out at the rover receiver.

Urban prediction scenarios. This research focused on models to predict the signal strength in a rural scenario and the effects of terrain. Since RTK GPS is also used in urban situations, models predicting the signal strength in urban scenarios could also be implemented into an RTK GPS mission planning tool.

The accuracy of various DTMs and their effect on wave propagation models. In researching this project no documentation was found describing the effect of error in DTMs on the predictions. Research to quantify and qualify how the accuracy o of a DTM affects the wave propagation models should be completed.

5.4 Concluding Remarks

This investigation has illustrated that current wave propagation models could be implemented into an RTK GPS mission planning tool for rural scenarios. To date no

GPS vendor has developed such a tool using any of the models described in this paper. This type of tool would provide the RTK GPS user with information vital to an RTK GPS survey in the office, potentially reducing wasted field time and therefore saving time and money.

For the geomatics community, the communications planning software industry opens a door for expertise in the areas of digital terrain models (production and use) and other related geographic information, such as remotely sensed data.

REFERENCES

Atlantis (2000). *Generation of DTED 2 over CFB Gagetown using ERS-1/2 SAR Interferometry Version 1*, Atlantic Scientific Inc, Nepean, Ontario, Canada.

AWE Communications (n.d.a). *ProMan: WinProp Prediction Tool User Reference*, AWE Communications, Gartringen, Germany.

AWE Communications (n.d.b). *Einbindung des Ausbreitungsmodells mit der Methode der Parabolischen Gleichung in ein Programmpaket zur Funknetzplanung* (Integration of Parabolic Equation in a Software Package for Radionetwork planning), AWE Communications, Gartringen, Germany.

AWE Communications (n.d.c). *Untersuchungen zur Berechnung terrestrischer Wellenausbreitung mit der Methode der Parabolischen Gleichung* (Analysis of the computation of terrestrial waves with the Parabolic Equation Method), AWE Communications, Gartringen, Germany.

AWE (2001). AWE Communications Homepage, Retrieved 23 April 2001 from the World Wide Web, www.awe-communications.com/index.html.

Bock, Y. (1995). "Reference Systems." In *GPS for Geodesy*, Ed. Kleusberg, A. and Teunissen, P., Netherlands Geodetic Commission, Delft, The Netherlands.

Chouinard, G., Breton, B., Paiement, R., and Voyer, R. (1996). "CRC-COV: A Software Program to Design and Predict DAB Coverage." Communications Research Centre, Ottawa, ON, Canada.

Coolen J. and Roddy D. (1995). *Electronic Communications.* Prentice-Hall, New Jersey, USA.

CRC (1994). *The CRC VHF/UHF Prediction Program*, May 1994, author unknown.

CRC (2001). CRC-COV Homepage, Retrieved 23 April 2001 from World Wide Web. www.drb.crc.ca/crc-cov/.

Dockery, G.D. (1988). "Modelling Electromagnetic Wave Propagation in the Troposphere Using the Parabolic Equation.", *IEEE Transactions on Antennas and Propagation*, Vol. 36, No. 10., pp. 1464-1470.

DMA (1996). *Performance Specification for Digital Terrain Elevation Data (DTED).* MIL-PRF-8920A, Department of Defense, Washington, US.

Egli, J. J. (1957). "Radio Propagation Above 40 MC Over Irregular Terrain." *Proceedings of IRE*, Vol. 45, Oct 1957, pp. 1383-1391.

El-Mowafy., A. (2000). "Performance Analysis of the RTK Technique in an Urban Environment." *The Australian Surveyor*, Vol. 45, No. 1, pp. 47-54.

Federal Standard 1037C (2000). *Telecommunications: Glossary of Telecommunication Terms.* , General Services Administration Information Technology Service. Retrieved 15 January 2000 from the World Wide Web. http://glossary.its.bldrdoc.gov/fs-1037/.

Feynman, R.P., Leighton, R.B., and Sands, M. (1964). "The Feynman Lectures on Physics: Volume II", Addison-Wesley Publishing Company Inc., New York, USA.

Giancoli, D.C. (1985). *Physics.* Prentice-Hall Canada, Toronto, ON, Canada.

Hata, M. (1980). "Empirical Formula for Propagation Loss in Land Mobile Radio Services", *IEEE Transactions on Vehicular Technology*, Vol VT-29, No.3, pp. 317-325.

Hatch, R., Jung, J., Enge, P., and Pervan, B. (2000). "Civilian GPS: The Benefits of Three Frequencies." *GPS Solutions*, Vol. 3, No. 4, pp. 1-9.

Hess, G. (1998). *Handbook of Land-Mobile Radio System Coverage*, Artech House Inc. Boston, USA.

Hoffman-Wellenhof, B., Lichtenegger, H., and Collins, J. (1997). *GPS Theory and Practice*. Fourth Edition, Springer Wien, New York, USA.

IEEE (1983). *IEEE Standard Definitions of Terms for Antennas*, The Institute of Electrical and Electronics Engineers, New York, USA.

IEEE (1988) "Coverage Prediction for Mobile Radio Systems Operating in the 800/900 MHz Frequency Range", IEEE Vehicular Society Committee on Radio Propagation, *IEEE Transactions on Vehicular Technology*, Vol. VT-37, No. 1, February 1988 pp. 3-72.

Kim D. and Langley R.B. (1999). "An optimized least-squares technique for improving ambiguity resolution performance and computational efficiency." *Proceedings of ION GPS'99*, Nashville, Tennessee, September 14-17, pp. 1579-1588.

Kuttler, J.R. and Dockery, G.D. (1991). "Theoretical description of the parabolic

approximation/Fourier split-step method of representing electromagnetic propagation in the troposphere.", *Radio Science*, Vol. 26., No. 2, pp. 381-393.

Langely, R.B. (1998). "RTK GPS", *GPS World*, Vol. 9, No. 9, pp. 70-75.

Langely, R.B. (1999). "Communication Links for DGPS", *GPS World*, Vol. 10, No. 5, pp 52-59.

Levy M.F., (1990) "Parabolic Equation Modelling of Propagation Over Irregular Terrain." *Electronic Letters*, Vol.26, No.15, pp 1153-1154.

Levy, M. (2000). *Parabolic Equation Methods for Electromagnetic Wave Propagation.* The Institution of Electrical Engineers, London, UK.

Magellan Corporation (2000). "SSRadio." Equipment brochure, Santa Clara, CA, USA.

Myint-U, T. (1980). "Partial Differential Equations of Mathematical Physics." Second Edition, North Holland, New York, USA.

Natural Resources Canada (NRC) (1993). *GPS Positioning Guide.* Natural Resources Canada, Ottawa, ON, Canada.

Okumura, T., Ohmori, E., and Fukuda, K. (1968). "Field Strength and Its Variability in VHF and UHF Land Mobile Service." *Review Electrical Communication Laboratory*, Vol 16, No. 9-10, pp 825-873.

Pacific Crest Corporation (1999). "Positioning Data Link." Equipment brochure, Santa Clara, CA, USA.

Pacific Crest Corporation (2000). *The Guide to Wireless GPS Links.* Pacific Crest Corporation, Santa Clara, USA.

Parkinson B.W. and Enge P.K. (1996). "Differential GPS." From *The Global Positioning System: Theory and Applications Volume 2*, Eds. Parkinson B.W. and Spilker J.J., American Institute of Aeronautics, USA.

Parsons, D. (1992). *The Mobile Radio Propagation Channel.* Pentech Press, London, UK.

Radio Technical Commission for Maritime Services (RTCM) (1998). "RTCM Recommended Standards for Differential GNSS (Global Navigation Satellite Systems) Service, Version 2.2." RTCM Paper 11-98/SC-104-STD, RTCM Special Committee No.104, Alexandria, Virginia.

Rappaport T.S. (1996) *Wireless Communications: Principles and Practice.* IEEE Press, New York, New York.

Sandhoo, K., Turner, D., and Shaw, M. (2000). "Modernizing of the Global Positioning System", *Proceedings of ION GPS 2000*, 19-22 September 2000, Salt Lake City, UT, pp. 2175-2183.

Talbot, N. C. (1996). "Compact Data Transmission Standard for High-Precision GPS." *Proceedings of the 9th International Technical Meeting of the Satellite Division ION GPS 1996*, Kansas City Convention Center, Kansas City, Missouri, September 17-20, pp. 86-871.

Trimble Navigation Limited (1997). "TRIMARK IIe Base/Repeater." Equipment brochure, Sunnyvale, CA, USA.

Trimble Navigation Limited (1998a). "Trimmark IIe Base/Repeater Operation Manual." Trimple Navigation Limited, Sunnyvale, CA, USA.

Van Dierendonck, A.J. and Hegarty C. (2000). "The New L5 Civil GPS Signal.", *GPS World*, Vol. 11, No. 9, pp 64-71.

Varner, C.C., (2000). *DGPS Carrier Phase Networks and Partial Derivative Algorithms.* Ph.D. dissertation, Department of Geomatics Engineering, University of Calgary, Calgary, AB, Canada.

Walker R.A. and Kubik K. (n.d.). "Parabolic Equation Modelling of GPS Signal Propagation and RF Communications Links in the Open Cut Mining Environment", Space Centre for Satellite Navigation Queensland University of Technology, Brisbane, Australia.

Walker R.A. and Sang J (n.d.). "Mission Planning for High Precision RTK GPS Surveying Using Accurate Digital Terrain Information", Space Centre for Satellite Navigation Queensland University of Technology, Brisbane, Australia.

Whitteker, J.H., (1990). "Fresenel-Kirchoff theory applied to terrain diffraction problems." *Radio Science*, Vol. 25, No. 5, pp 837-851.

Whitteker, J.H., (1994). "Physical Optics and Terrain Diffraction." *Radioscientist*, Vol. 5, No. 3, pp 111-116.

Yacoub, M.D. (1993). *Foundations of Mobile Radio Engineering*, CRC Press, London, UK.

APPENDIX A

Transmitting Power Calculations

Base Station Information	
Make:	Trimble TRIMMARK IIe Base
Amplifier Power:	25 Watts
Antenna Gain:	5 dBi
Cable loss/100 ft:	12 dB
Cable length:	6 feet
Transmitting Frequency:	450 MHz

The communication planning software required the effective radiated power (ERP) transmitting power as an input. The transmitting power included any system losses and antenna gain. The calculation for the transmitting power is as follows:

ERP = Amp Power (dBW) + Ant Gain (dBd) – Cable loss (dB)

Amp Power = 10 log 25
= 13.98 dBW

Ant Gain (dBd) = Ant Gain (dBi) – 2.15
= 5 – 2.15
= 2.85 dBd (with respect to a dipole)

Cable loss = 6 ft * 12 dB/100 ft
= 0.72 dB

ERP = 13.98 + 2.85 – 0.72
= 16.11 dBW

ERP (Watts) = 40.83 Watts

APPENDIX B

Standard Deviation of Predicted Received Power

Standard deviation of predicted received power.

Test area terrain statistics from DTED model.	
Terrain Average Height:	117.6 m
Standard deviation of terrain height:	38.5 m
Δh:	148 (Hills)

The following table shows the standard deviation from each recommendations in Section 2.2.3.3 (Table 2-1) and a transmitting frequency of 450 MHz.

Egli:	15.3 dB
Hufford and Montgomery:	11.6 dB
Longley-Rice:	12.1 dB
CCIR:	10-15 dB

Using a value of 10 dB from CCIR the average of all four models is 12.3, therefore for this project a standard deviation of 12 dB will be used for all models.

APPENDIX C

Data Work Flow

CRC-COV Data Work Flow

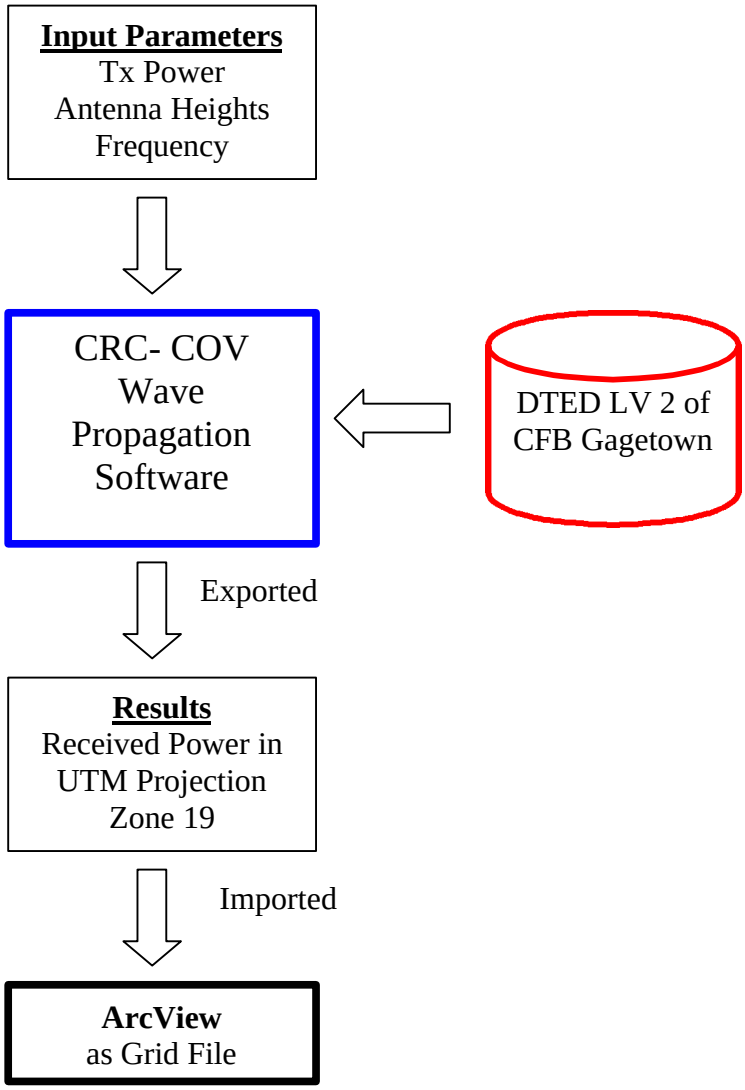

WinProp Data Work Flow

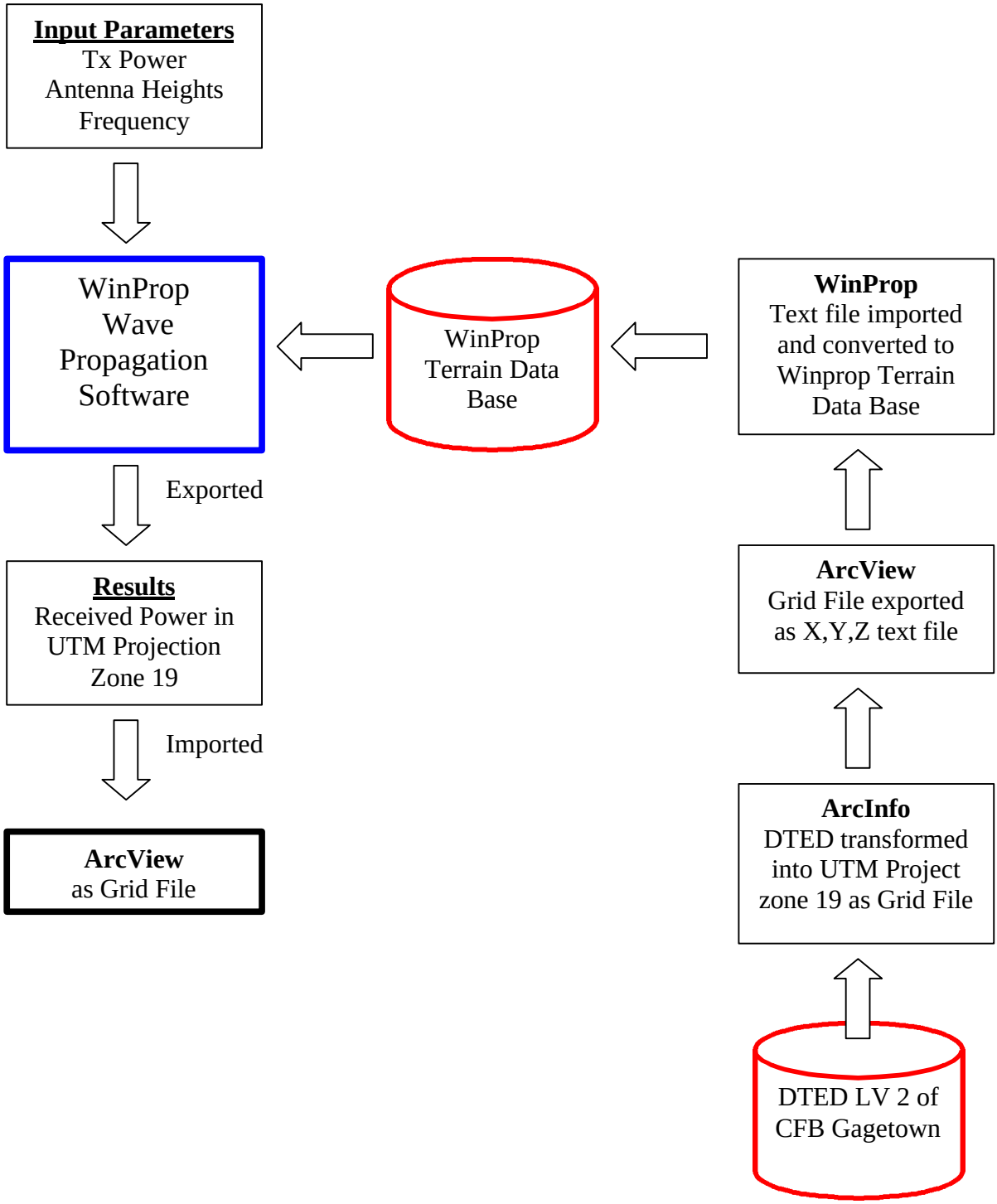

VITA

Michael Kenneth Hogan

Royal Military College: Bachelor of Science and Engineering 1996

Publications: Nil

Conference Presentations: Digital Earth 2001